CHAPTER 19

Block Coded Modulation

Combining block coding and channel signal sets to construct bandwidth-efficient codes is referred to as *block coded modulation* (BCM). Codes constructed by this combination are called BCM (or block coded modulation) codes, analogous to TCM codes. BCM codes are much easier to construct (or design) than TCM codes. The most powerful method for constructing BCM codes is the *multilevel coding technique* devised by Imai and Hirakawa in 1976 [1]. This chapter is devoted to the multilevel construction of BCM codes and multistage decoding of these codes. Also presented are concatenated coded modulation and product coded modulation for achieving large coding gains and high spectral efficiencies with reduced decoding complexity, and multilevel coded modulation for unequal error protection.

19.1 DISTANCE CONCEPTS

Let s be a point $(X(s), Y(s))$ in a two-dimensional Euclidean space R^2 with x- and y-coordinates $X(s)$ and $Y(s)$, respectively. Let s and s' be two points in R^2. The squared Euclidean (SE) distance between s and s', denoted by $d_E^2(s, s')$, is defined as

$$d_E^2(s, s') \triangleq (X(s) - X(s'))^2 + (Y(s) - Y(s'))^2.$$

Let $\mathbf{v} = (s_0, s_1, \ldots, s_{n-1})$ and $\mathbf{v}' = (s_0', s_1', \ldots, s_{n-1}')$ be two n-tuples over R^2. Then, the squared Euclidean distance between $\mathbf{v}$ and $\mathbf{v}'$, denoted by $d_E^2(\mathbf{v}, \mathbf{v}')$, is defined as

$$d_E^2(\mathbf{v}, \mathbf{v}') \triangleq \sum_{i=0}^{n-1} (X(s_i) - X(s_i'))^2 + (Y(s_i) - Y(s_i'))^2.$$

Let S be a two-dimensional modulation signal set (or signal space). Each signal $s \in S$ is represented as a point $(X(s), Y(s))$ in R^2. An n-tuple over S is simply a sequence of n signals from S. A BCM code C of length n over the signal space S is simply a collection of n-tuples over S. The minimum squared Euclidean (MSE) distance of C, denoted by $d_E^2[C]$, is defined as

$$d_E^2[C] \triangleq \min\{d_E^2(\mathbf{v}, \mathbf{v}') : \mathbf{v}, \mathbf{v}' \in C \text{ and } \mathbf{v} \neq \mathbf{v}'\}. \tag{19.1}$$

The minimum Hamming distance of the code, $d_H[C]$, is also called the *minimum symbol distance* of the code in coded modulation. For two codewords $\mathbf{v} = (s_0, s_1, \ldots, s_{n-1})$ and $\mathbf{v}' = (s_0', s_1', \ldots, s_{n-1}')$ in C, the *product distance* between $\mathbf{v}$ and $\mathbf{v}'$, denoted by $d_P^2(\mathbf{v}, \mathbf{v}')$, is defined as

$$d_P^2(\mathbf{v}, \mathbf{v}') \triangleq \prod_{i=0, s_i \neq s_i'}^{n-1} d_E^2(s_i, s_i'). \tag{19.2}$$

The *minimum product distance* of the code, $d_P^2[C]$, is defined as

$$d_P^2[C] \triangleq \min\{d_P^2(\mathbb{v}, \mathbb{v}') : \mathbb{v}, \mathbb{v}' \in C \text{ and } d_H(\mathbb{v}, \mathbb{v}') = d_H[C]\}. \tag{19.3}$$

For an AWGN channel, the error performance of a modulation code depends primarily on its MSE distance and path multiplicity. For the fading channels, such as Rayleigh or Ricean channels, the error performance of a modulation code depends primarily on its minimal symbol and minimal product distances and path multiplicity (nearest neighbors) [29]. It depends on the MSE distance to a lesser degree. These distances are called the *distance parameters* of the code.

If every message of k information bits is encoded into a codeword in C, the spectral efficiency of the code is

$$\eta[C] = \frac{k}{n} \text{ bits/symbol.}$$

Assume that the channel is an AWGN channel and all the codewords are equally likely to be transmitted. Let $\mathbb{r} = (x_0, y_0, x_1, y_1, \ldots, x_{n-1}, y_{n-1})$ be the output sequence of the receiver demodulator, where x_i and y_i are the x- and y-coordinates of the ith received signal r_i. For maximum likelihood decoding, the received sequence $\mathbb{r}$ is decoded into a codeword $\mathbb{v}^*$ such that

$$d_E^2(\mathbb{v}^*, \mathbb{r}) < d_E^2(\mathbb{v}_i, \mathbb{r}),$$

for $\mathbb{v}_i \neq \mathbb{v}^*$.

19.2 MULTILEVEL BLOCK MODULATION CODES

Multilevel coding [1] is a very powerful technique for constructing bandwidth-efficient modulation codes systematically with arbitrarily large distance parameters from Hamming distance component (block or convolutional) codes in conjunction with a proper bits-to-signal mapping through signal set partitioning. It provides the flexibility to coordinate the distance parameters of a code to attain the best performance for a given channel. Furthermore, the multilevel codes constructed by this method allow the use of multistage decoding procedures that provide good trade-off between error performance and decoding complexity.

Multilevel coding is best explained by constructing a class of 3-level BCM codes over the 8-PSK signal set with unit energy. For bits-to-signal mapping, each 8-PSK signal s is labeled by a sequence of 3 bits, $a_0a_1a_2$, based on the 3-level binary partition chain 8-PSK/QPSK/BPSK/{0}, as shown in Figure 18.12. For convenience, the partition chain is reproduced in Figure 19.1. (*Note:* The order of bit labeling given here is the opposite of that given in Figure 18.12.) Let $Q(a_0)$ denote the set of signal points in S whose labels have a_0 as the prefix. $Q(a_0)$ forms a QPSK. Let $Q(a_0a_1)$ denote the set of two signal points in S whose labels have a_0a_1 as the prefix. Each $Q(a_0a_1)$ is a BPSK. Let $Q(a_0a_1a_2)$ denote the set that contains the signal point s in S labeled with $a_0a_1a_2$. The intraset distances Δ_0^2, Δ_1^2, Δ_2^2, and Δ_3 of S, $Q(a_0)$, $Q(a_0a_1)$, and $Q(a_0a_1a_2)$ are 0.586, 2, 4, and ∞, respectively. The signal set partition and signal labeling process define a one-to-one mapping $f(\cdot)$ that maps each label $a_0a_1a_2$ into its corresponding signal point s; that is, $f(a_0a_1a_2) = s$.

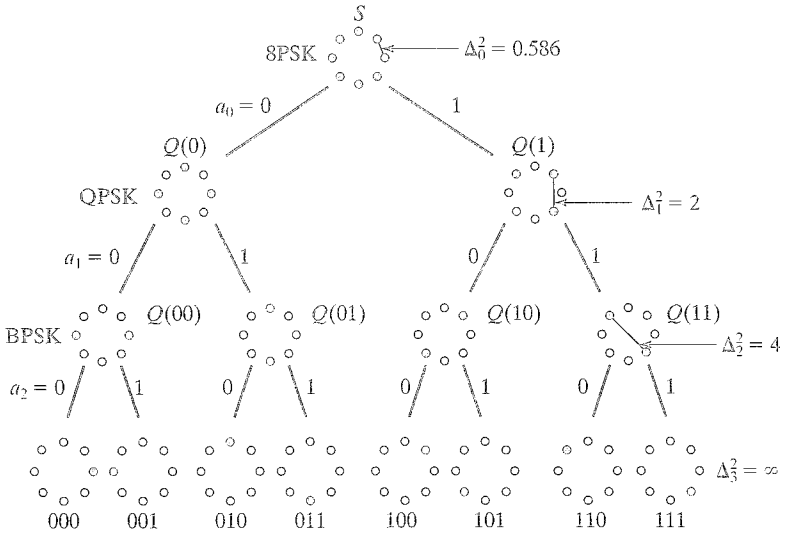

FIGURE 19.1: 8-PSK/QPSK/BPSK/{0} partition chain and signal labeling.

For $0 \leq i \leq 2$, let C_i be a binary (n, k_i, d_i) linear block code of length n, dimension k_i, and minimum Hamming distance d_i. Let

$$\begin{aligned} \mathbb{v}_0 &= (v_{0,0}, v_{0,1}, \ldots, v_{0,j}, \ldots, v_{0,n-1}), \\ \mathbb{v}_1 &= (v_{1,0}, v_{1,1}, \ldots, v_{1,j}, \ldots, v_{1,n-1}), \\ \mathbb{v}_2 &= (v_{2,0}, v_{2,1}, \ldots, v_{2,j}, \ldots, v_{2,n-1}), \end{aligned}$$

be three codewords in C_0, C_1, and C_2, respectively. We form the following sequence:

$$\mathbb{v}_0 * \mathbb{v}_1 * \mathbb{v}_2 \stackrel{\Delta}{=} (v_{0,0}v_{1,0}v_{2,0}, \ldots, v_{0,j}v_{1,j}v_{2,j}, \ldots, v_{0,n-1}v_{1,n-1}v_{2,n-1}). \quad (19.4)$$

This sequence is simply obtained by interleaving the three codewords $\mathbb{v}_0$, $\mathbb{v}_1$, and $\mathbb{v}_2$. For $0 \leq j < n$, we take $v_{0,j}v_{1,j}v_{2,j}$ as the label for a signal point in the 8-PSK signal space S. Then,

$$f(\mathbb{v}_0 * \mathbb{v}_1 * \mathbb{v}_2) \stackrel{\Delta}{=} (f(v_{0,0}v_{1,0}v_{2,0}), f(v_{0,1}v_{1,1}v_{2,1}), \ldots, f(v_{0,n-1}v_{1,n-1}v_{2,n-1})) \quad (19.5)$$

is a sequence of n 8-PSK signals. Let

$$\begin{aligned} C &\stackrel{\Delta}{=} f[C_0 * C_1 * C_2] \\ &= \{f(\mathbb{v}_0 * \mathbb{v}_1 * \mathbb{v}_2) : \mathbb{v}_i \in C_i \text{ for } 0 \leq i \leq 2\}. \end{aligned} \quad (19.6)$$

Then, C is a 3-level 8-PSK modulation code of length n and dimension $k = k_0 + k_1 + k_2$. The code consists of 2^k signal sequences. Because $k_0 + k_1 + k_2$ information bits are encoded into a code sequence of n 8-PSK signals, the spectral efficiency of the code is

$$\eta[C] = \frac{k_0 + k_1 + k_2}{n} \text{ bits/symbol.}$$

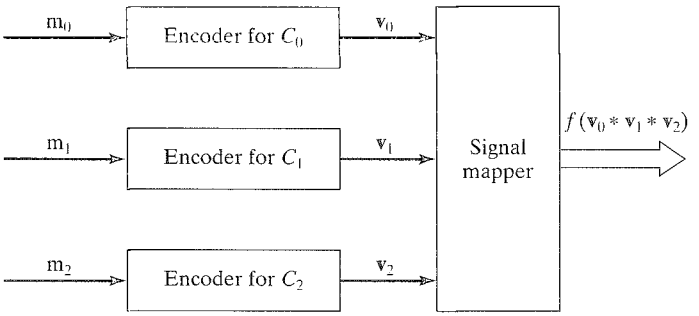

FIGURE 19.2: An encoder for a 3-level BCM code.

In this construction of a 3-level 8-PSK code, each binary component code contributes a labeling bit. An encoder for such code is shown in Figure 19.2. In encoding, the first component codeword $v_0 = (v_{0,0}, v_{0,1}, \ldots, v_{0,n-1})$ simply selects a sequence of n QPSK signal sets $(Q(v_{0,0}), Q(v_{0,1}), \ldots, Q(v_{0,n-1}))$. From this sequence of QPSK signal sets, the second component codeword $v_1 = (v_{1,0}, v_{1,1}, \ldots, v_{1,n-1})$ selects a sequence of n BPSK signal sets $(Q(v_{0,0}v_{1,0}), Q(v_{0,1}v_{1,1}), \ldots, Q(v_{0,n-1}v_{1,n-1}))$, where for $0 \leq j < n$,

$$Q(v_{0,j}v_{1,j}) \subset Q(v_{0,j}).$$

Then, the third component codeword $v_2 = (v_{2,0}, v_{2,1}, \ldots, v_{2,n-1})$ selects a sequence of n signal points $(Q(v_{0,0}v_{1,0}v_{2,0}), Q(v_{0,1}v_{1,1}v_{2,1}), \ldots, Q(v_{0,n-1}v_{1,n-1}v_{2,n-1}))$ from the BPSK sequence $(Q(v_{0,0}v_{1,0}), Q(v_{0,1}v_{1,1}), \ldots, Q(v_{0,n-1}v_{1,n-1}))$, with $Q(v_{0,j}v_{1,j}v_{2,j}) \in Q(v_{0,j}v_{1,j})$ for $0 \leq j < n$. This sequence is the output signal sequence. With this view of the encoding operation, the encoder of Figure 19.2 can be reconfigured as shown in Figure 19.3.

The MSE distance of a 3-level 8-PSK BCM code is given by Theorem 19.1.

THEOREM 19.1 The MSE distance $d_E^2[C]$ of the 3-level 8-PSK block modulation code $C = f[C_0 * C_1 * C_2]$ defined by (19.6) is lower bounded as follows:

$$d_E^2[C] \geq \min\{0.586 \times d_0, 2 \times d_1, 4 \times d_2\}. \tag{19.7}$$

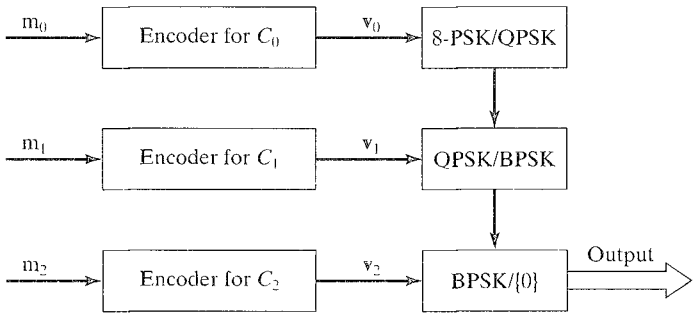

FIGURE 19.3: Another encoder configuration for a 3-level 8-PSK BCM code.

Proof. Let $f(\mathbf{v}_0 * \mathbf{v}_1 * \mathbf{v}_2)$ and $f(\mathbf{v}'_0 * \mathbf{v}'_1 * \mathbf{v}'_2)$ be two different signal sequences in C. To determine the squared Euclidean distance between these two signal sequences, we must consider three cases.

For the first case, suppose $\mathbf{v}_0 \neq \mathbf{v}'_0$. Because the minimum Hamming distance of C_0 is d_0, $\mathbf{v}_0$ and $\mathbf{v}'_0$ must differ in at least d_0 places. At each of these places, the labels of the corresponding signals in $f(\mathbf{v}_0 * \mathbf{v}_1 * \mathbf{v}_2)$ and $f(\mathbf{v}'_0 * \mathbf{v}'_1 * \mathbf{v}'_2)$ differ in the first labeling bit. Because $f(\cdot)$ is a one-to-one mapping, $f(\mathbf{v}_0 * \mathbf{v}_1 * \mathbf{v}_2)$ and $f(\mathbf{v}'_0 * \mathbf{v}'_1 * \mathbf{v}'_2)$ must differ in these places. In the 8-PSK signal constellation with unit energy, two signals whose labels differ in the first labeling bit are separated by a squared Euclidean distance of at least $\Delta_0^2 = 0.586$. Consequently,

$$d_E^2(f(\mathbf{v}_0 * \mathbf{v}_1 * \mathbf{v}_2), f(\mathbf{v}'_0 * \mathbf{v}'_1 * \mathbf{v}'_2)) \geq 0.586 \times d_0. \tag{19.8}$$

For the second case, suppose $\mathbf{v}_0 = \mathbf{v}'_0$, and $\mathbf{v}_1 \neq \mathbf{v}'_1$. Because the minimum Hamming distance of C_1 is d_1, $\mathbf{v}_1$ and $\mathbf{v}'_1$ must differ in at least d_1 places. At each of these places the labels of the corresponding signals in $f(\mathbf{v}_0 * \mathbf{v}_1 * \mathbf{v}_2)$ and $f(\mathbf{v}'_0 * \mathbf{v}'_1 * \mathbf{v}'_2)$ are identical at the first labeling bit but differ in the second labeling bit. These two signals in the 8-PSK signal constellation must be separated by a squared Euclidean distance of at least $\Delta_1^2 = 2$. Therefore, the squared Euclidean distance between $f(\mathbf{v}_0 * \mathbf{v}_1 * \mathbf{v}_2)$ and $f(\mathbf{v}'_0 * \mathbf{v}'_1 * \mathbf{v}'_2)$ must be at least $2 \times d_1$; that is,

$$d_E^2(f(\mathbf{v}_0 * \mathbf{v}_1 * \mathbf{v}_2), f(\mathbf{v}'_0 * \mathbf{v}'_1 * \mathbf{v}_2)) \geq 2 \times d_1. \tag{19.9}$$

The last case is that $\mathbf{v}_0 = \mathbf{v}'_0$, $\mathbf{v}_1 = \mathbf{v}'_1$, and $\mathbf{v}_2 \neq \mathbf{v}'_2$. Because the minimum Hamming distance of C_2 is d_2, $\mathbf{v}_2$ and $\mathbf{v}'_2$ must differ in at least d_2 places. This implies that $f(\mathbf{v}_0 * \mathbf{v}_1 * \mathbf{v}_2)$ and $f(\mathbf{v}'_0 * \mathbf{v}'_1 * \mathbf{v}'_2)$ differ in at least d_2 places. At each of these places the labels of the two corresponding signals are identical at the first two labeling bits but differ in the third bit. These two signals must be in the same BPSK signal set and separated by a squared Euclidean distance $\Delta_2^2 = 4$. Consequently,

$$d_E^2(f(\mathbf{v}_0 * \mathbf{v}_1 * \mathbf{v}_2), f(\mathbf{v}'_0 * \mathbf{v}'_1 * \mathbf{v}'_2)) \geq 4 \times d_2. \tag{19.10}$$

Combining (19.8), (19.9), and (19.10), we have

$$d_E^2(f(\mathbf{v}_0 * \mathbf{v}_1 * \mathbf{v}_2), f(\mathbf{v}'_0 * \mathbf{v}'_1 * \mathbf{v}'_2)) \geq \min\{0.586 \times d_0, 2 \times d_1, 4 \times d_2\}.$$

This result implies the bound of (19.7). Q.E.D.

EXAMPLE 19.1

Suppose we want to construct a 3-level 8-PSK BCM code C of length $n = 8$, with MSE distance $d_E^2[C] = 4$ and spectral efficiency $\eta[C] = 2$ bits/symbol. It follows from Theorem 19.1 (19.7) that the minimum Hamming distances of three binary component codes must be 8, 2, and 1, respectively. To achieve 2 bits/symbol spectral efficiency, the sum $k_0 + k_1 + k_2$ of dimensions of three component codes must be 16. Under these conditions, the three binary component codes may be chosen as follows:

1. C_0 is the (8, 1, 8) repetition code that consists of the all-zero and all-one vectors.
2. C_1 is the (8, 7, 2) even-parity-check (or SPC) code that consists of all the even-weight 8-tuples over $GF(2)$.
3. C_2 is the (8, 8, 1) universal code that consists of all the 8-tuples over $GF(2)$.

Then, $C = f[C_0 * C_1 * C_2]$ is a 3-level 8-PSK BCM code of length $n = 8$ and MSE distance

$$d_E^2[C] \geq \min\{0.586 \times 8, 2 \times 2, 4 \times 1\} = 4.$$

In fact, $d_E^2[C] = 4$ (see Problem 19.1). Because $k_0 + k_1 + k_2 = 1 + 7 + 8 = 16$, the spectral efficiency is $\eta[C] = 16/8 = 2$ bits/symbol. This 8-PSK BCM code has the same MSE distance and spectral efficiency as the 8-PSK TCM code (code 2) given in Example 18.4. It achieves a 3-dB asymptotic coding gain over the uncoded QPSK system with the same spectral efficiency.

This code also has a very simple trellis structure. To construct the trellis for C, we first construct the trellises for the component codes. The trellises for the three component codes are shown in Figure 19.4. Taking the Cartesian product of these three trellises, we obtain the trellis of the interleaved code $C_0 * C_1 * C_2$, as shown in Figure 19.5. Then, we map each branch label into an 8-PSK signal based on the partition and labeling shown in Figure 19.1. The result is the trellis for the 3-level 8-PSK code C shown in Figure 19.6. It consists of two parallel and structurally identical 2-state subtrellises. The code is phase invariant under multiples of 45° rotation [7]. Its bit-error performance with Viterbi decoding is shown in Figure 19.7. It achieves a 2-dB real coding gain over the uncoded QPSK at a BER of 10^{-6}.

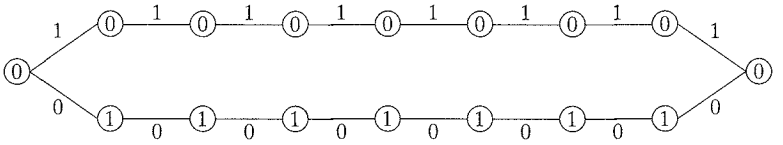

(a) An 8-section trellis for the (8, 1, 8) repetition code C_0

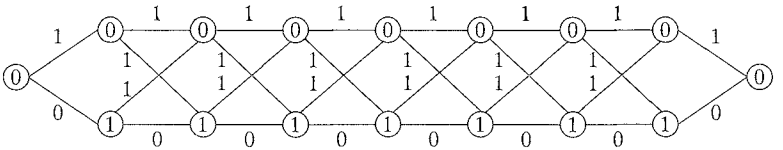

(b) An 8-section trellis for the (8, 7, 2) even-parity-check code C_1

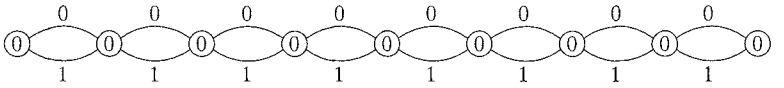

(c) An 8-section trellis for the (8, 8, 1) universal code C_2

FIGURE 19.4: Trellises for the binary component codes.

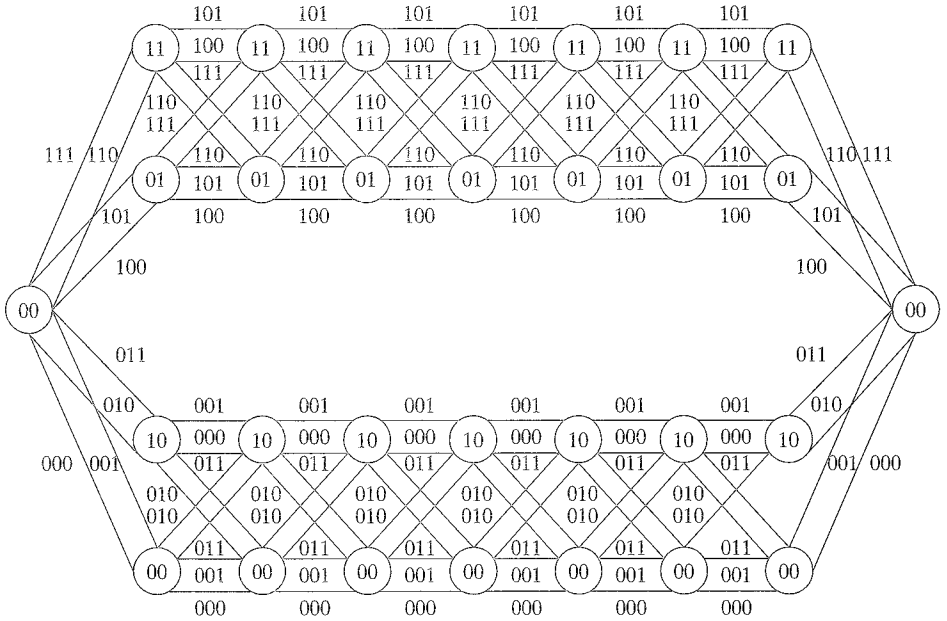

FIGURE 19.5: Eight-section trellis for the interleaved code $(8, 1, 8) * (8, 7, 2) * (8, 1, 1)$.

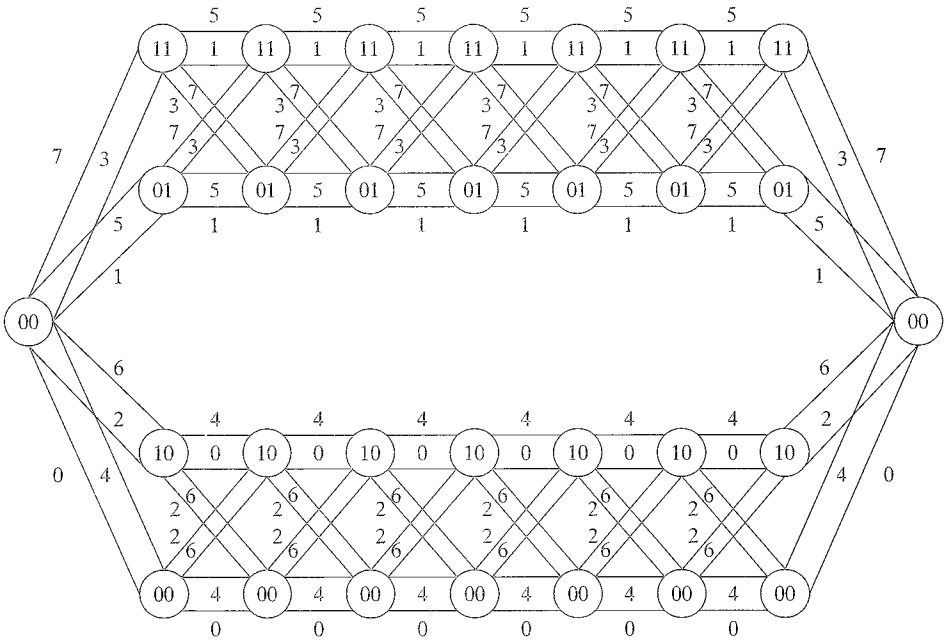

FIGURE 19.6: Eight-section trellis for the 3-level 8-PSK code $f[(8, 1, 8) * (8, 7, 2) * (8, 1, 1)]$.

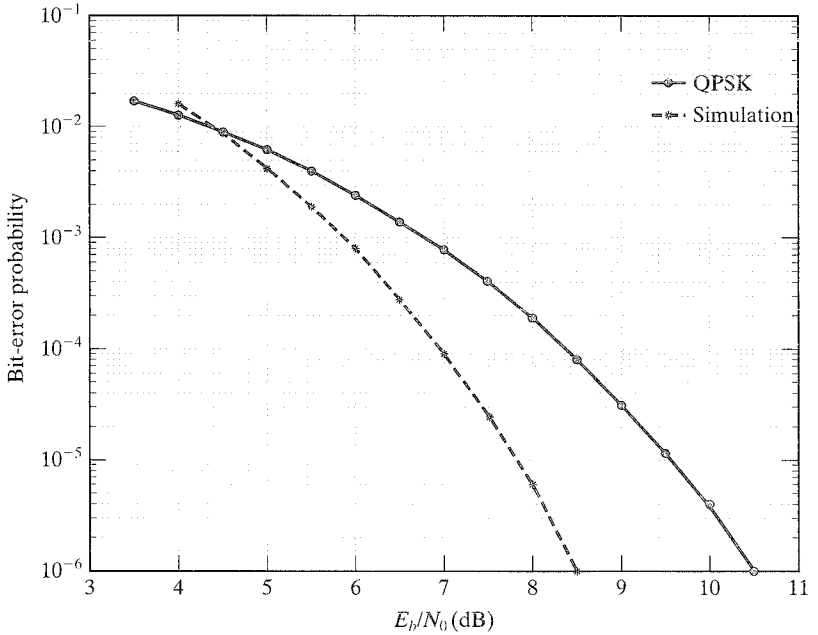

FIGURE 19.7: Bit-error performance of the 3-level 8-PSK BCM code $f[(8, 1, 8) * (8, 7, 2) * (8, 8, 1)]$.

The preceding example shows that Theorem 19.1 (or (19.7)) can be used as a guideline for constructing good 3-level 8-PSK BCM codes for an AWGN channel. For a given MSE distance, the three component codes should be chosen to maximize the spectral efficiency and minimize the decoding complexity.

The other two distance parameters of a 3-level 8-PSK BCM code are given in Theorem 19.2 [9].

THEOREM 19.2 Consider a 3-level 8-PSK BCM code $C = f[C_0 * C_1 * C_2]$ with component codes C_0, C_1, and C_2, whose minimum Hamming distances are d_0, d_1, and d_2, respectively. Let Δ_0^2, Δ_1^2, and Δ_2^2 be the intraset distances at the three levels of the partition chain 8-PSK/QPSK/BPSK, respectively. Then, the minimum symbol distance $d_H[C]$ and the minimum product distance $d_P^2[C]$ are given by

1.
$$d_H[C] = \min\{d_i : 0 \le i \le 2\}, \tag{19.11}$$

2. Let q be the smallest integer in the index set $I = \{0, 1, 2\}$ for which $d_q = d_H[C]$. Then,
$$d_P^2[C] = (\Delta_q^2)^{d_q}. \tag{19.12}$$

Proof. The proof of the first part, (19.11), is similar to the proof of the MSE distance $d_E^2[C]$ given in Theorem 19.1.

The proof of the second part of the theorem is as follows. For $0 \leq j \leq 2$, let $\mathbf{v}^{(j)} = (v_0^{(j)}, v_0^{(j)}, \cdots, v_{n-1}^{(j)})$ denote a codeword in the component code C_j. Because q is the smallest integer in $I = \{0, 1, 2\}$ for which $d_q = d_H[C]$, there must exist two codewords, $\mathbf{v}^{(q)}$ and $\hat{\mathbf{v}}^{(q)}$, in C_q such that the Hamming distance between them is

$$d_H(\mathbf{v}^{(q)}, \hat{\mathbf{v}}^{(q)}) = d_q = d_H[C].$$

Consider two signal sequences, $\mathbf{x} = f(\mathbf{v}^{(0)} * \mathbf{v}^{(1)} * \mathbf{v}^{(2)})$ and $\hat{\mathbf{x}} = f(\hat{\mathbf{v}}^{(0)} * \hat{\mathbf{v}}^{(1)} * \hat{\mathbf{v}}^{(2)})$, in C such that $d_H(\mathbf{v}^{(q)}, \hat{\mathbf{v}}^{(q)}) = d_q = d_H[C]$, and $\mathbf{v}^{(j)} = \hat{\mathbf{v}}^{(j)}$ for $j \neq q$. These two signal sequences differ in exactly d_q places. At each of these d_q places, the labels of two corresponding signals in $\mathbf{x}$ and $\hat{\mathbf{x}}$ are identical in every label bit except for the qth label bit. Based on the 8-PSK/QPSK/BPSK partition and signal labeling shown in Figure 19.1, the squared Euclidean distance between these two corresponding signals is equal to the intraset distance Δ_q^2 at the qth partition level. Consequently, it follows from the definition of product distance given by (19.2) that the product distance between $\mathbf{x}$ and $\hat{\mathbf{x}}$ is

$$d_P^2(\mathbf{x}, \hat{\mathbf{x}}) = (\Delta_q^2)^{d_q}.$$

This implies that $d_P^2[C] \leq (\Delta_q^2)^{d_q}$. In the following, we prove that $d_P^2[C] < (\Delta_q^2)^{d_q}$ cannot be true.

Without loss of generality, we assume $q = 1$. Then, $d_0 > d_1$, and $d_2 \geq d_1$. Suppose $d_P^2[C] < (\Delta_q^2)^{d_q}$. Then, there exist two signal sequences,

$$\mathbf{y} = f(\mathbf{v}^{(0)} * \mathbf{v}^{(1)} * \mathbf{v}^{(2)}) = (y_0, y_0, \cdots, y_{n-1})$$

and

$$\hat{\mathbf{y}} = f(\hat{\mathbf{v}}^{(0)} * \hat{\mathbf{v}}^{(1)} * \hat{\mathbf{v}}^{(2)}) = (\hat{y}_0, \hat{y}_0, \cdots, \hat{y}_{n-1}),$$

in C such that $d_H(\mathbf{y}, \hat{\mathbf{y}}) = d_1 = d_H[C]$ and

$$d_P^2(\mathbf{y}, \hat{\mathbf{y}}) = \prod_{\substack{i=0 \\ y_i \neq \hat{y}_i}}^{n-1} d_E^2(y_i, \hat{y}_i) < (\Delta_1^2)^{d_1}. \tag{19.13}$$

This implies that there is a j such that

$$d_E^2(y_j, \hat{y}_j) < \Delta_1^2. \tag{19.14}$$

Because $y_j = f(v_j^{(0)} v_j^{(1)} v_j^{(2)})$ and $\hat{y}_j = f(\hat{v}_j^{(0)} \hat{v}_j^{(1)} \hat{v}_j^{(2)})$, the inequality of (19.14) implies that $v_j^{(0)} \neq \hat{v}_j^{(0)}$ and $\mathbf{v}^{(0)} \neq \hat{\mathbf{v}}^{(0)}$. Let $\mathbf{z} = f(\hat{\mathbf{v}}^{(0)} * \mathbf{v}^{(1)} * \mathbf{v}^{(2)})$. Then, we can readily see that

$$d_H(\mathbf{y}, \hat{\mathbf{y}}) \geq d_H(\mathbf{y}, \mathbf{z}). \tag{19.15}$$

Because $\mathbf{v}^{(0)} \neq \hat{\mathbf{v}}^{(0)}$, $d_H(\mathbf{y}, \mathbf{z}) \geq d_0$. It follows from (19.15) that

$$d_H(\mathbf{y}, \hat{\mathbf{y}}) \geq d_0 > d_1,$$

which contradicts the fact that $d_H(\mathbf{y}, \hat{\mathbf{y}}) = d_1$. Hence, the hypothesis, $d_P^2[C] < (\Delta_1^2)^{d_1}$, does not hold, and we must have $d_P^2[C] = (\Delta_1^2)^{d_1}$. This concludes the proof. Q.E.D.

EXAMPLE 19.2

Suppose we want to construct a 3-level 8-PSK code with minimum symbol distance 4, minimum product distance of at least 4, and spectral efficiency around 2 bits/symbol. From (19.11) we find that the smallest minimum Hamming distance of the component codes must be 4. From (19.12) we find that for a minimum product distance of at least 4, the first component code cannot be the code with the smallest minimum Hamming distance. In this case, we should choose either the second or the third component code to have the smallest Hamming distance. Possible choices of the component codes are

1. C_0 is the (32, 16, 8) second-order RM code of length 32.
2. C_1 is the third-order (32, 26, 4) RM code of length 32.
3. C_2 is the same as C_1; that is, $C_2 = C_1$.

The resultant 3-level 8-PSK code, $C = f[C_0 * C_1 * C_2]$, has the following distance parameters: $d_E^2[C] = 4.688$, $d_H[C] = 4$, $d_P^2[C] = 16$, and $\eta[C] = 2.125$ bits/symbol.

The construction and developments of 3-level 8-PSK codes can be generalized to multilevel codes over any M-ary PSK or QAM signal set. Let S be either an MPSK or a QAM signal space with 2^l signal points. We form a binary partition chain $S/S_1/\cdots/S_l$ for the signal space S, where $S_1, S_2, \cdots, S_l = \{0\}$ are subspaces of S, and S_i consists of 2^{l-i} points for $1 \le i \le l$. For $0 \le i \le l$, let Δ_i^2 denote the intraset distance at the ith level of partition. For $i = 0$, Δ_0^2 is the intraset distance of the signal space S. The partition of S is carried out such that the intraset distances increase monotonically, that is,

$$\Delta_0^2 \le \Delta_1^2 \le \cdots \le \Delta_l^2. \tag{19.16}$$

Based on this partition chain, each of the 2^l signal points in S is labeled by a unique binary string of length l, denoted by $a_0a_1\cdots a_{l-1}$. This signal labeling defines a one-to-one bits-to-signal mapping $f(\cdot)$. For each label $a_0a_1\cdots a_{l-1}$, $f(a_0a_1\cdots a_{l-1})$ is its corresponding signal. For $1 \le i \le l$, let $Q(a_0a_1\cdots a_{i-1})$ denote the set of 2^{l-i} signal points in S whose labels have $a_0a_1\cdots a_{i-1}$ as the common prefix. The intraset distance of $Q(a_0a_1\cdots a_{i-1})$ is Δ_i^2.

An l-level BCM code over a signal space (MPSK or QAM) with 2^l signal points is constructed in the same manner as a 3-level 8-PSK BCM code. For $0 \le i < l$, let C_i be a binary (n, k_i, d_i) linear block code of length n, dimension k_i, and minimum Hamming distance d_i. Let

$$\begin{aligned}
\mathbf{v}_0 &= (v_{0,0}, v_{0,1}, \cdots, v_{0,j}, \cdots, v_{0,n-1}),\\
\mathbf{v}_1 &= (v_{1,0}, v_{1,1}, \cdots, v_{1,j}, \cdots, v_{1,n-1}),\\
&\vdots\\
\mathbf{v}_{l-1} &= (v_{l-1,0}, v_{l-1,1}, \cdots, v_{l-1,j}, \cdots, v_{l-1,n-1}),
\end{aligned}$$

be l codewords in $C_0, C_1, \cdots, C_{l-1}$, respectively. We interleave these l codewords to form the following sequence:

$$\begin{aligned}
\mathbf{v}_0 * \mathbf{v}_1 * \cdots * \mathbf{v}_{l-1} = (&v_{0,0}v_{1,0}\cdots v_{l-1,0}, \cdots, v_{0,j}v_{1,j}\cdots\\
&v_{l-1,j}, \cdots, v_{0,n-1}v_{1,n-1}\cdots v_{l-1,n-1}).
\end{aligned}$$

For $0 \le j < n$, we take $v_{0,j}v_{1,j}\cdots v_{l-1,j}$ as the label of a signal point $s \in S$. Then,

$$f(\mathbb{v}_0 * \mathbb{v}_1 * \cdots * \mathbb{v}_{l-1}) = (f(v_{0,0}v_{1,0}\cdots v_{l-1,0}), \cdots, f(v_{0,j}v_{1,j}\cdots v_{l-1,j}), \cdots, f(v_{0,n-1}v_{1,n-1}\cdots v_{l-1,n-1}))$$

is a sequence of n signals from the signal space S. Then,

$$\begin{aligned} C &\stackrel{\Delta}{=} f[C_0 * C_1 * \cdots * C_{l-1}] \\ &= \{f(\mathbb{v}_0 * \mathbb{v}_1 * \cdots * \mathbb{v}_{l-1}) : \mathbb{v}_i \in C_i \text{ for } 0 \le i < l\} \end{aligned} \tag{19.17}$$

is an l-level BCM code over S with dimension $k = k_0 + k_1 + \cdots + k_{l-1}$. Because all the component codes are linear, the interleaved code $C_0 * C_1 * \cdots * C_{l-1}$ is linear. For this reason we may regard the BCM code $C = f[C_0 * C_1 * \cdots * C_{l-1}]$ as a linear code. The distance parameters of this code are characterized by Theorem 19.3, which is simply a generalization of Theorems 19.1 and 19.2.

THEOREM 19.3 Let S be either an MPSK or a QAM signal space with 2^l signals. Let $d_E^2[C]$, $d_H[C]$, and $d_P^2[C]$ be the MSE distance, minimum symbol distance, and minimum product distance of an l-level BCM code over S, respectively. Then,

1.
$$d_E^2[C] \ge \min\{d_i \Delta_i^2 : 0 \le i < l\}; \tag{19.18}$$

2.
$$d_H[C] = \min\{d_i : 0 \le i < l\}. \tag{19.19}$$

3. Let q be the smallest integer in the index set $I = \{0, 1, \cdots, l-1\}$ for which $d_q = d_H[C]$. Then,
$$d_P^2[C] = (\Delta_q^2)^{d_q}, \tag{19.20}$$

where $\Delta_0^2, \Delta_1^2, \cdots, \Delta_{l-1}^2$ are the intraset distances of the partition chain $S/S_1/\cdots/S_l = \{0\}$.

The construction of an l-level BCM code over a signal space S with 2^l signal points consists of four steps:

1. Label each signal point in S with a unique binary string of l bits through a binary partition chain for S.
2. Choose l binary component codes, $C_0, C_1, \cdots, C_{l-1}$.
3. Interleave the component codes.
4. Map each interleaved sequence, $\mathbb{v}_0 * \mathbb{v}_1 * \cdots * \mathbb{v}_{l-1}$, at step 3 into a signal sequence $f(\mathbb{v}_0 * \mathbb{v}_1 * \cdots * \mathbb{v}_{l-1})$ over S.

An n-section trellis for an l-level code, $C = f[C_0 * C_1 * \cdots * C_{l-1}]$, over S can be constructed in two steps. For $0 \le i < l$, let $T^{(i)}$ be the n-section bit-level trellis for the

ith binary component code C_i. We construct an n-section trellis T for the interleaved code $C_0 * C_1 * \cdots * C_{l-1}$ by taking the Cartesian product of $T^{(0)}, T^{(1)}, \cdots, T^{(l-1)}$ and labeling each branch in T with l bits. These l bits form a label for a signal point in S. We map each branch label in T into a signal point in S. The result is an n-section signal-level trellis for the l-level code $C = f[C_0 * C_1 * \cdots * C_{l-1}]$ over S.

EXAMPLE 19.3

Suppose we want to construct a 4-level 16-QAM code with MSE distance $8\Delta_0^2$ and spectral efficiency around 3 bits/symbol. The 4-level binary partition chain for 16-QAM is shown in Figure 19.8. For $i = 0, 1, 2$, $\Delta_{i+1}^2 = 2\Delta_i^2$, a possible choice of the component codes is

1. C_0 is the (16, 5, 8) first-order RM code of length 16.
2. C_1 is the (16, 11, 4) second-order RM code of length 16.
3. C_2 is the (16, 15, 2) SPC code of length 16.
4. C_3 is the (16, 16, 1) universal code.

The resultant 4-level 16-QAM code, $C = f[C_0 * C_1 * C_2 * C_3]$, has the following parameters: $d_E^2[C] = 8\Delta_0^2$, and $\eta[C] = 2.9375$ bits/symbol.

Multilevel coded modulation systems can also be designed using convolutional codes (or a combination of block and convolutional codes) as component codes.

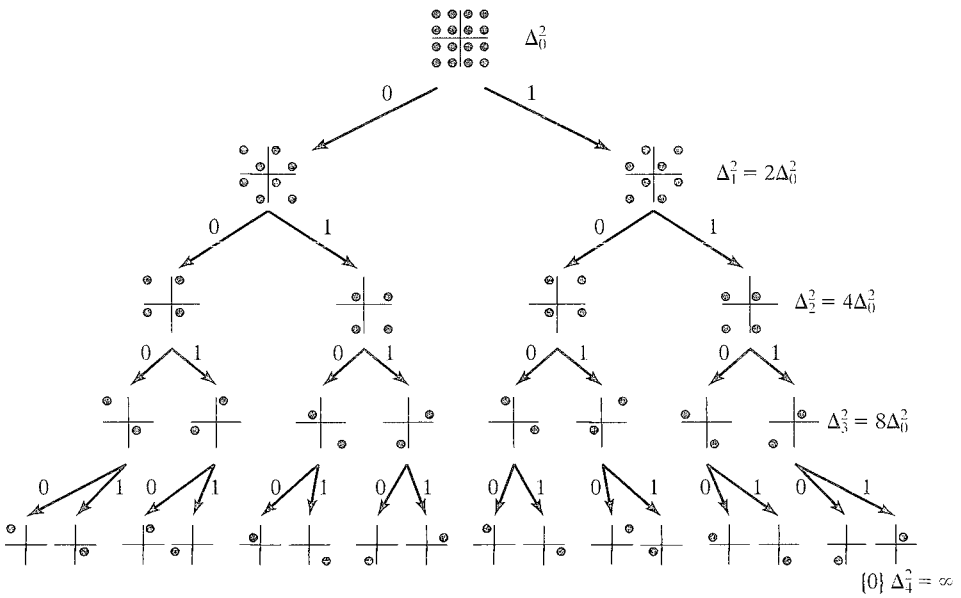

FIGURE 19.8: The 4-level binary partition chain for 16-QAM.

19.3 MULTISTAGE DECODING OF MULTILEVEL BCM CODES

For short BCM codes, maximum likelihood decoding can be implemented based on their full code trellises using a trellis-based decoding algorithm. The trellises of long BCM codes, may be too complex for practical implementation of any trellis-based MLD algorithm; however, the multilevel structure of these codes allows the use of multistage decoding that provides an effective trade-off between error performance and decoding complexity [6, 11, 12, 16].

In multistage soft-decision decoding of a multilevel BCM code, component codes are decoded with soft-decision MLD, one at a time, stage by stage, as described in Section 15.3. The decoded information at each stage is passed to the next stage. The decoding process begins with the first-level component code and ends at the last-level component code.

For simplicity, the decoding process is explained by using a 3-level 8-PSK BCM code $C = f[C_0 * C_1 * C_2]$. Assume an AWGN channel. Let $\mathbb{r} = (r_0, r_0, \cdots, r_{n-1})$ be the received sequence at the output of the demodulator, where for $0 \leq i < n$

$$r_i = (x_i, y_i) \in R^2.$$

19.3.1 First-Stage Decoding

Let $\mathbb{v}_0 = (v_{0,0}, v_{0,1}, \cdots, v_{0,n-1})$ be a codeword in C_0. Let $d_E^2[r_i, Q(v_{0,i})]$ be the MSE distance between the ith received symbol and the signal points in $Q(v_{0,i})$. The SE distance between the received sequence $\mathbb{r}$ and the codeword $\mathbb{v}_0$ is defined as

$$d_E^2(\mathbb{r}, \mathbb{v}_0) \triangleq \sum_{i=0}^{n-1} d_E^2[r_i, Q(v_{0,i})]. \tag{19.21}$$

For every codeword $\mathbb{v}_0 \in C_0$, we compute the distance $d_E^2(\mathbb{r}, \mathbb{v}_0)$ and decode $\mathbb{r}$ into the codeword $\hat{\mathbb{v}}_0 = (\hat{v}_{0,0}, \hat{v}_{0,1}, \cdots, \hat{v}_{0,n-1})$ for which $d_E^2(\mathbb{r}, \hat{\mathbb{v}}_0)$ is minimum. This concludes the first-stage decoding.

19.3.2 Second-Stage Decoding

The decoded information, $\hat{\mathbb{v}}_0$, at the first-stage decoding is passed to the second stage. Let $\mathbb{v}_1 = (v_{1,0}, v_{1,1}, \cdots, v_{1,n-1})$ be a codeword in C_1. Let $d_E^2[r_i, Q(\hat{v}_{0,i} v_{1,i})]$ be the MSE distance between the ith received symbol r_i and the signal points in $Q(\hat{v}_{0,i} v_{1,i})$. For every codeword $\mathbb{v}_1 \in C_1$, we compute the distance

$$d_E^2(\mathbb{r}, \hat{\mathbb{v}}_0 * \mathbb{v}_1) \triangleq \sum_{i=0}^{n-1} d_E^2[r_i, Q(\hat{v}_{0,i} v_{1,i})]. \tag{19.22}$$

Then, we decode $\mathbb{r}$ into the codeword $\hat{\mathbb{v}}_1$ in C_1 for which $d_E^2(\mathbb{r}, \hat{\mathbb{v}}_0 * \hat{\mathbb{v}}_1)$ is minimum. This completes the second-stage decoding.

19.3.3 Third-Stage Decoding

The decoded information at the first and second stages, $\hat{\mathbb{v}}_0$ and $\hat{\mathbb{v}}_1$, is made available to the third decoding stage. For every codeword $\mathbb{v}_2 \in C_2$, we compute

the distance

$$d_E^2(\mathbb{r}, \hat{\mathbb{v}}_0 * \hat{\mathbb{v}}_1 * \mathbb{v}_2) \triangleq \sum_{i=0}^{n-1} d_E^2[r_i, Q(\hat{v}_{0,i}\hat{v}_{1,i}v_{2,i})]$$
$$= \sum_{i=0}^{n-1} d_E^2[r_i, f(\hat{v}_{0,i}\hat{v}_{1,i}v_{2,i})]. \tag{19.23}$$

We decode $\mathbb{r}$ into the codeword $\hat{\mathbb{v}}_2 \in C_2$ for which $d_E^2(\mathbb{r}, \hat{\mathbb{v}}_0 * \hat{\mathbb{v}}_1 * \hat{\mathbb{v}}_2)$ is minimum. This completes the entire decoding process, and $\{\hat{\mathbb{v}}_0, \hat{\mathbb{v}}_1, \hat{\mathbb{v}}_2\}$ forms the decoded set. A decoder is shown in Figure 19.9.

The foregoing multistage decoding is known as the *closest coset decoding*. A trellis-based MLD algorithm can be used for decoding each component code. The entire decoding complexity is the sum of decoding complexities of the component codes. Owing to the possibility of error propagation from one stage to the next, the preceding multistage decoding algorithm is not optimum even though each stage of decoding is MLD; it is suboptimum.

EXAMPLE 19.4

Consider a 3-level 8-PSK BCM code, $C = f[C_0 * C_1 * C_2]$, of length $n = 32$, where (1) C_0 is the first-order (32, 6, 16) RM code, (2) C_1 is the third-order (32, 26, 4) RM code, and (3) C_2 is the (32, 31, 2) even-parity-check code. The total number of information bits is $k = 6 + 26 + 31 = 63$. Therefore, the spectral efficiency of C is $\eta[C] = 63/32 = 1.96875$ bits/symbol (almost 2 bits/symbol). From (19.7) we find

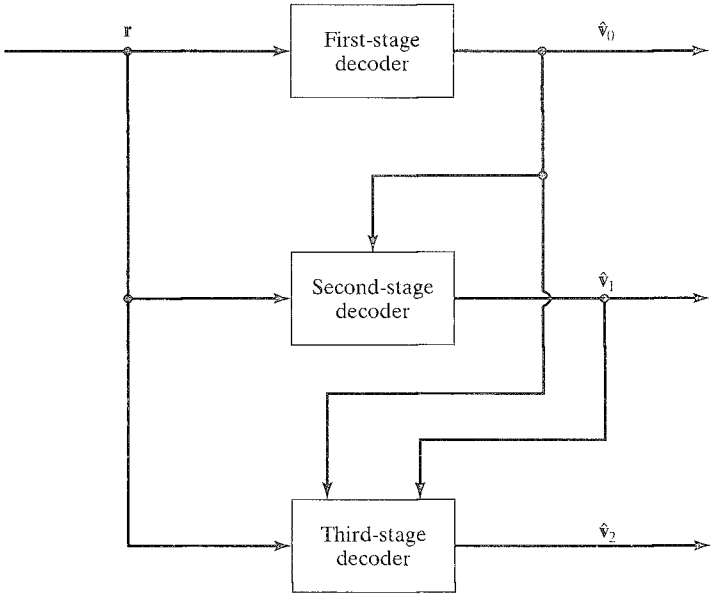

FIGURE 19.9: A three-stage decoder for a 3-level BCM code.

that the MSE distance of C is $d_E^2[C] = 8$. This 3-level 8-PSK code has almost the same spectral efficiency as the uncoded QPSK, 2 bits/symbol. It achieves a 6-dB asymptotic coding gain over the uncoded QPSK with optimal MLD.

The first component code C_0 has a 4-section 16-state trellis. The second component code C_1 also has a 4-section 16-state trellis. The third component code has a 32-section 2-state trellis. The Cartesian product of the three trellises would result in a 4-section trellis with 512 states. Decoding based on this overall trellis is rather complicated; however, three-stage suboptimum decoding of this BCM code makes the decoding relatively much less complex. The bit-error performance of this code with 3-stage suboptimum decoding is shown in Figure 19.10. There is a 3.6-dB real coding gain over the uncoded QPSK at a BER of 10^{-6}.

The 3-stage decoding of a 3-level BCM code can be generalized in a straightforward manner to l-stage decoding of an l-level BCM code, $C = f[C_0 * C_1 * \cdots * C_{l-1}]$, over a signal space S. For $0 \leq j < l$, let

$$\hat{\mathbf{v}}_0 = (\hat{v}_{0,0}, \hat{v}_{0,1}, \cdots, \hat{v}_{0,n-1})$$

$$\hat{\mathbf{v}}_1 = (\hat{v}_{1,0}, \hat{v}_{1,1}, \cdots, \hat{v}_{1,n-1})$$

$$\vdots$$

$$\hat{\mathbf{v}}_{j-1} = (\hat{v}_{j-1,0}, \hat{v}_{j-1,1}, \cdots, \hat{v}_{j-1,n-1})$$

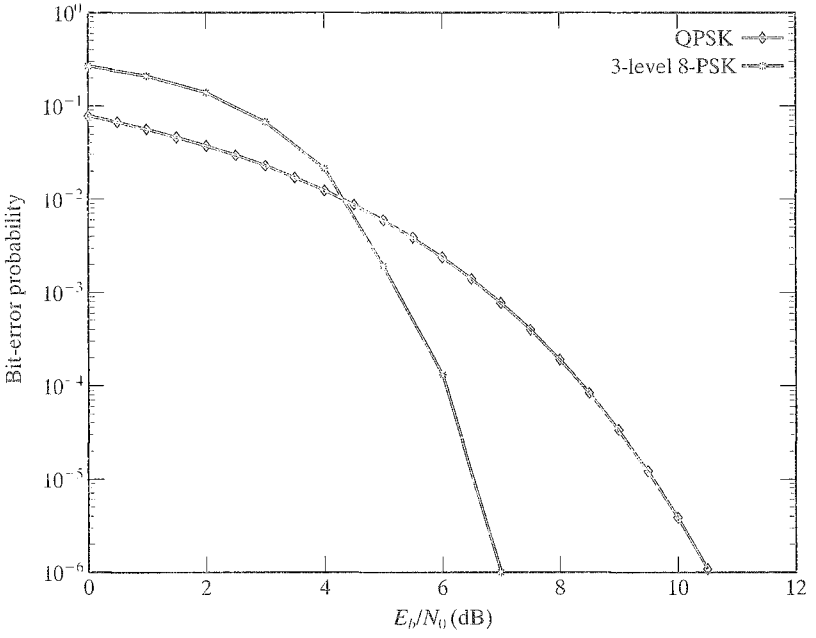

FIGURE 19.10: Bit-error performance of the 3-level 8-PSK code $f[(32, 6) * (32, 26) * (32, 31)]$.

be the decoded codewords of the first j stages. For every codeword $\mathbb{v}_j = (v_{j,0}, v_{j,1}, \cdots, v_{j,n-1}) \in C_j$, we compute the distance

$$d_E^2(\mathbb{r}, \hat{\mathbb{v}}_0 * \hat{\mathbb{v}}_1 * \cdots * \hat{\mathbb{v}}_{j-1} * \mathbb{v}_j) \triangleq \sum_{i=0}^{n-1} d_E^2[r_i, Q(\hat{v}_{0,i}\hat{v}_{1,i}, \cdots, \hat{v}_{j-1,i}v_{j,i})], \quad (19.24)$$

where $d_E^2[r_i, Q(\hat{v}_{0,i}\hat{v}_{1,i}, \cdots, \hat{v}_{j-1,i}v_{j,i})]$ denotes the MSE distance between the ith received symbol r_i and the signal points in $Q(\hat{v}_{0,i}\hat{v}_{1,i}, \cdots, \hat{v}_{j-1,i}v_{j,i})$. Then, the $(j+1)$th stage decoding decodes $\mathbb{r}$ into codeword $\hat{\mathbb{v}}_j$ in C_j for which $d_E^2(\mathbb{r}, \hat{\mathbb{v}}_0 * \hat{\mathbb{v}}_1 * \cdots * \hat{\mathbb{v}}_{j-1} * \hat{\mathbb{v}}_j)$ is minimum. Decoding stops at the lth stage.

EXAMPLE 19.5

Consider a 4-level 16-QAM BCM code, $C = f[C_0 * C_1 * C_2 * C_3]$, of length $n = 16$, where (1) C_0 is the first-order (16, 5, 8) RM code, (2) C_1 is the second-order (16, 11, 4) RM code, (3) C_2 is the (16, 15, 2) even-parity-check code, and (4) C_3 is the (16, 16, 1) universal code. The total number of information bits is $k = 5 + 11 + 15 + 16 = 47$. Therefore, the spectral efficiency of C is $\eta[C] = 47/16 = 2.9375$ bits/symbol (almost 3 bits/symbol). From (19.18) we find that the MSE distance of C is $d_E^2[C] = 8\Delta_0^2$. This 4-level 16-QAM code has almost the same spectral efficiency as the uncoded 8-AM-PM constellation obtained at the first partitioning level of Figure 19.8, which achieves 3 bits/symbol. Hence, it achieves a 6-dB asymptotic coding gain over the uncoded 8-AM/PM with optimal MLD. The bit-error performance of this code with 4-stage suboptimum decoding is shown in Figure 19.11. There is a 2.8-dB real coding gain over the uncoded 8-AM/PM considered at a BER of 10^{-5}. Note that although the 16-QAM and 8-AM/PM constellations considered in this example have the same average energy, this is no longer the case in general, since several 8-point QAM constellations can be chosen as an uncoded reference. As a result, a given 8-point QAM constellation with the same average energy as the 16-QAM constellation has to be considered as an uncoded reference, which automatically determines the SE distance of this 8-AM/PM constellation.

An upper bound for each stage of multistage decoding of multilevel codes can be derived based on the union bound. First, consider a 2^l-PSK BCM code, and assume that the all-zero codeword is sent at level 1. Then, a decoding error at stage 1 is made if there exists $\hat{\mathbb{v}}_0 \neq \mathbb{0}$ with

$$d_E^2(\mathbb{r}, \hat{\mathbb{v}}_0) < d_E^2(\mathbb{r}, \mathbb{0}). \quad (19.25)$$

Let ω represent the Hamming weight of $\hat{\mathbb{v}}_0$. Then, for each nonzero position of $\hat{\mathbb{v}}_0$, each point in $Q(0)$ has two nearest neighbors in $Q(1)$ at SE distance Δ_0^2. Because at stage 1 of the decoding, it is assumed that any n-tuple is a valid codeword for the remaining stages, $\hat{\mathbb{v}}_0$ can be mapped into 2^ω sequences at SE distance $\omega\Delta_0^2$ from any given sequence of n points in $Q(0)$. Let $A_\omega^{(i)}$ represent the number of codewords of Hamming weight ω in code C_i used at level-i. It follows that the word-error

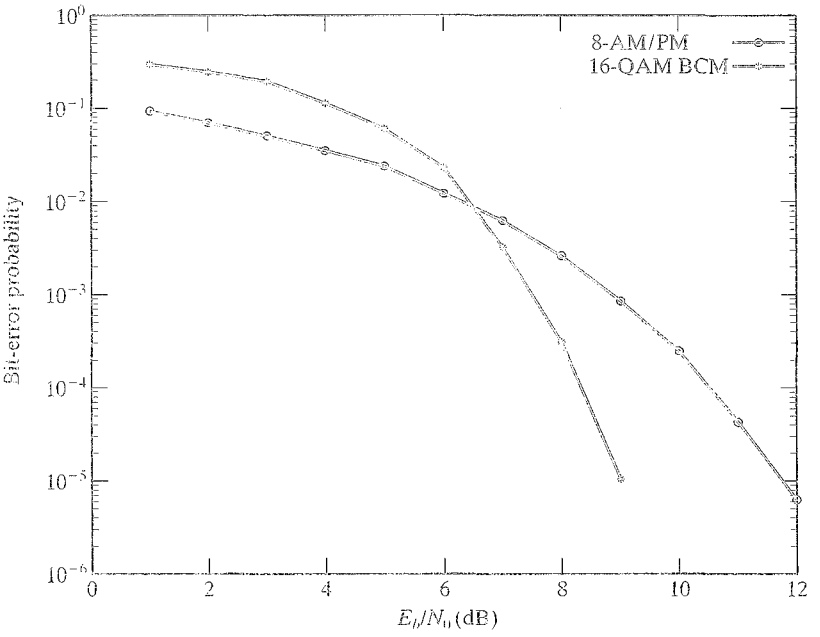

FIGURE 19.11: Bit-error performance of the 4-level 16-QAM code $f[(15, 5)*(16, 11)*(16, 15)*(16, 16)]$.

probability at stage 1 of the decoding is upper bounded by

$$P_{w,0} \leq \sum_{\omega=d_0}^{n} 2^{\omega} A_{\omega}^{(0)} Q\left(\sqrt{\frac{\eta[C]E_b\Delta_0^2}{2N_0}}\right). \tag{19.26}$$

In 2^l-PSK, for $1 \leq i < l$, each point $Q(a_0a_1\cdots a_{i-1}0)$ has two nearest neighbors at SE distance Δ_i^2 in $Q(a_0a_1\cdots a_{i-1}1)$ It follows that for $1 \leq i < l$, the word-error probability at stage-i of the decoding is upper bounded by

$$P_{w,i} \leq \sum_{\omega=d_i}^{n} 2^{\omega} A_{\omega}^{(i)} Q\left(\sqrt{\frac{\eta[C]E_b\Delta_i^2}{2N_0}}\right) + P_{w,i-1}, \tag{19.27}$$

where the term $P_{w,i-1}$ represents the probability of error propagation from stage-$(i-1)$ to stage-i when stage-$(i-1)$ is in error ($P_{\omega,0} = 0$). Finally, since the decoding of stage-l is the same as for BPSK, it follows that

$$P_{w,l-1} \leq \sum_{\omega=d_{l-1}}^{n} A_{\omega}^{(l)} Q\left(\sqrt{\frac{\eta[C]E_b\Delta_{l-1}^2}{2N_0}}\right) + P_{w,l-2}. \tag{19.28}$$

For the 3-level 8-PSK BCM code of Example 19.4, Figure 19.12 shows the union bound on $P_{w,l-1}$ computed from (19.27), which usually dominates the overall

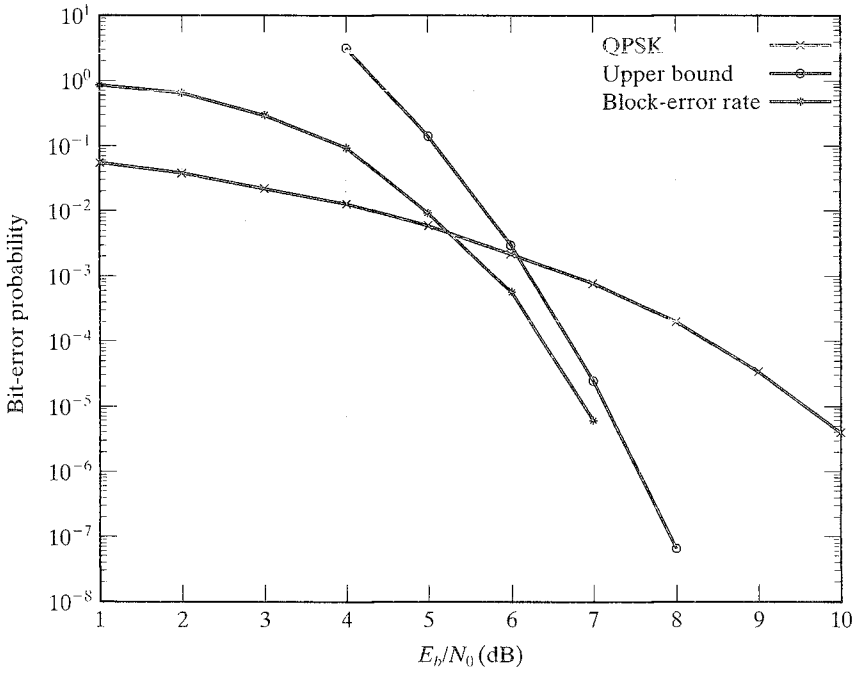

FIGURE 19.12: The union bound of the 3-level 8-PSK BCM code of Example 19.4.

union bound for multistage decoding of BCM codes. In general, when a powerful code C_0 is used al level 1, the union bound on $P_{w,1}$ tends to become quite loose at low-to-medium SNR values.

This analytical approach for 2^l-PSK BCM can be generalized for evaluating an upper bound for each stage of multistage decoding of multilevel codes in general. We define $N_{eff}^{(j)}$ as the average number of nearest neighbors at SE distance Δ_j^2 corresponding to stage-j of the partitioning. Then, it follows that for $0 \leq i < l$, the word-error probability at stage-i of the decoding is upper bounded by

$$P_{w,i} \leq \sum_{\omega=d_i}^{n} \left(N_{eff}^{(j)}\right)^{\omega} A_{\omega}^{(i)} Q\left(\sqrt{\frac{\eta[C]E_b\Delta_i^2}{2N_0}}\right) + P_{w,i-1}. \tag{19.29}$$

For the 4-level 16-QAM BCM code of Example 19.5, we find that

$$N_{eff}^{(1)} = (4 \cdot 4 + 3 \cdot 8 + 2 \cdot 4)/16, = 3, \tag{19.30}$$

$$N_{eff}^{(2)} = (1 \cdot 2 + 2 \cdot 4 + 4 \cdot 2)/8. = 2.25. \tag{19.31}$$

For this 16-QAM BCM code, Figure 19.13 depicts the union bound on $P_{w,1}$ computed from (19.29).

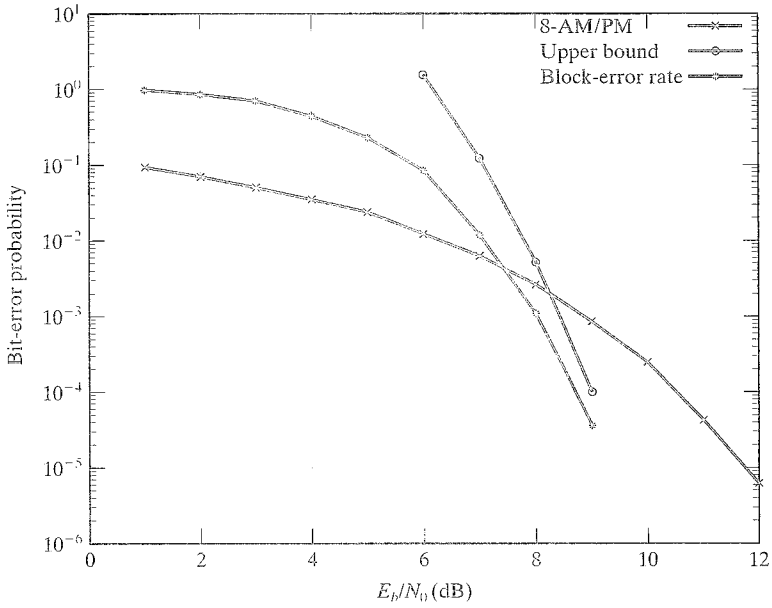

FIGURE 19.13: The union bound of the 16-QAM BCM code of Example 19.5.

19.4 CONCATENATED CODED MODULATION

Coded modulation can be used in conjunction with concatenated coding to achieve large coding gain, high reliability, and high spectral efficiency with reduced decoding complexity. This combination of two coding techniques is called *concatenated coded modulation* (CCM). CCM systems, either with one level or with multilevels, can be constructed in exactly the same manner as concatenated coding systems presented in Chapter 15, except that BCM codes are used as the inner codes.

19.4.1 Single-Level Concatenated Coded Modulation Systems

In a single-level CCM system, the outer code, denoted by B, is an (N, K) linear block code, say an RS code, with symbols from $GF(2^b)$. The inner code, denoted by A, is a multilevel BCM code of length n and dimension $k = \lambda b$ over a certain signal space S. The encoding consists of two stages. At the first stage of encoding, λ outer-code codewords are formed and stored in a buffer as a $\lambda b \times N$ array, as shown in Figure 19.14. Each column of the array is λb bits long and consists of λ code symbols, one from each outer-code codeword. At the second stage of encoding, each column of the array is encoded into a sequence of n signals in the signal space S based on the BCM inner code A. This signal sequence is then transmitted. The outer code is interleaved by a depth of λ.

The decoding also consists of two stages, the inner and outer decodings. When a sequence of n signals is received, it is decoded into λb bits based on the BCM inner code A using a soft-decision decoding algorithm, say, multistage decoding presented in the previous section. These λb bits are then stored as a column of a $\lambda b \times N$ array in a buffer for the second-stage decoding. After N inner code decodings, the received

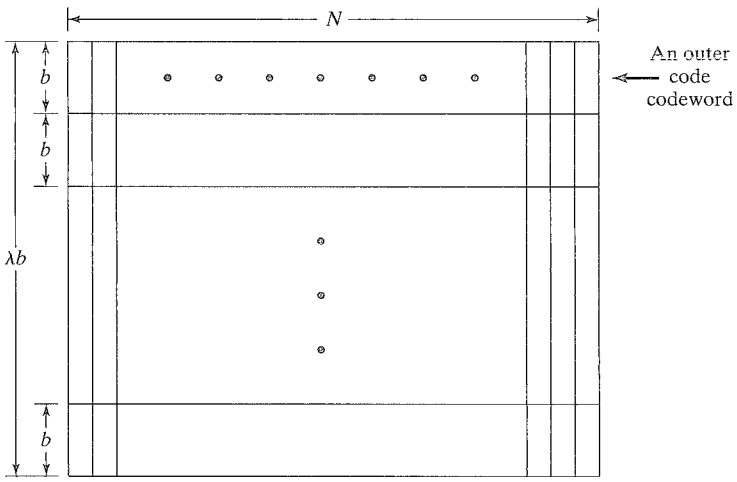

FIGURE 19.14: An array of λ outer code codewords.

buffer contains a $\lambda b \times N$ decoded array. Each column of this array consists of λ estimated symbols, one for each transmitted outer-code codeword. Therefore, the array contains λ received words for the outer code B, and they are decoded based on the outer code. To maintain low decoding complexity, the outer code is decoded with an algebraic decoding algorithm (or a reliability-based decoding algorithm).

EXAMPLE 19.6

For this example, the outer code B is the NASA standard (255, 223) RS code over $GF(2^8)$ with minimum Hamming distance 33 [13]. The inner code A is the 3-level 8-PSK BCM code of length $n = 8$ and dimension $k = 16$ constructed in Example 19.1. Because $k = 16$ and $b = 8, \lambda = 2$. Therefore, the outer code is interleaved by a depth of $\lambda = 2$. The spectral efficiency of the overall CCM system is $(223/255) \cdot \eta[A] = (223/255) \cdot 2 = 1.749$ bits/symbol. Figure 19.15 depicts the system. Because the inner code has a very simple 4-state trellis (see Figure 19.6), it is decoded with a Viterbi algorithm based on the full-code trellis. The outer RS code is decoded with the Euclidean decoding algorithm presented in Section 7.5. The error performance of this CCM system is shown in Figure 19.16. The system achieves a 5-dB coding gain over the uncoded QPSK at a BER of 10^{-6} with 14.3% bandwidth expansion. For SNR $E_b/N_0 = 6.2$ dB, the system practically provides error-free data transmission.

19.4.2 Multilevel Concatenated Coded Modulation Systems

In a q-level concatenated coded modulation system, q pairs of outer and inner codes are used. For $1 \leq i \leq q$, let B_i be an (N, K_i) linear block code over $GF(2^{m_i})$ with minimum Hamming distance D_i. These codes are used as the outer codes. The inner codes are constructed from a multilevel BCM code A_0 and a sequence of q subspaces of A_0.

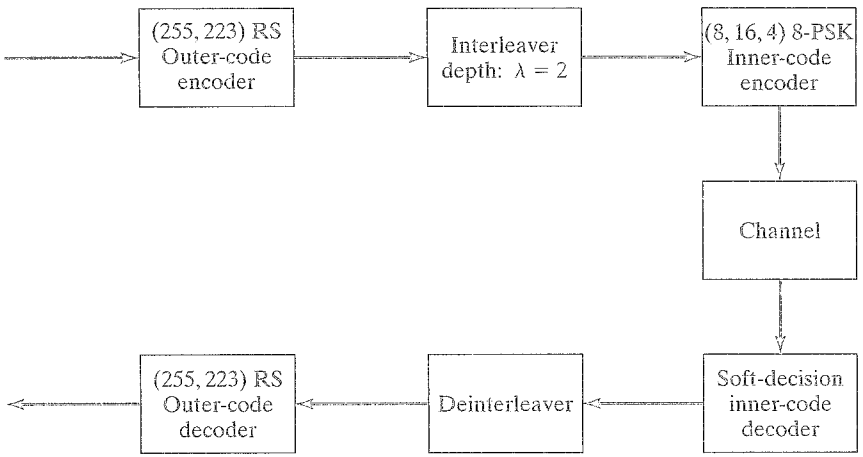

FIGURE 19.15: A single-level concatenated coded modulation system with the NASA standard (255, 223) RS code as the outer code and an (8, 16, 4) 8-PSK code as the inner code.

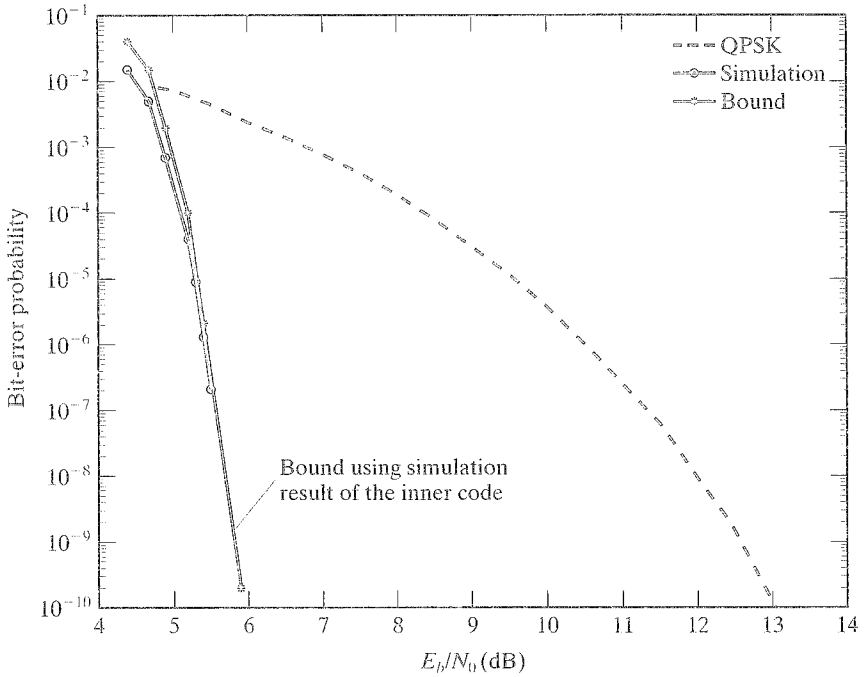

FIGURE 19.16: Bit-error performance of the single-level CCM system with the NASA standard (255, 223) RS code as the outer code and an (8, 16, 4) 3-level 8-PSK BCM code as the inner code.

Let $A_0 = f[C_0 * C_1 * \cdots * C_{l-1}]$ be an l-level BCM code over signal space S of length n, dimension k_0, and MSE distance $d_0^2 \triangleq d_E^2[A_0]$. We require that

$$k_0 = m_1 + m_2 + \cdots + m_q. \tag{19.32}$$

For $0 \le i < l$, let C_i' be a linear subcode of the ith component code C_i of A_0. Then, the interleaved code $C_0' * C_1' * \cdots * C_{l-1}'$ is a linear subcode of $C_0 * C_1 * \cdots * C_{l-1}$. After bits-to-signal mapping based on $f(\cdot)$, $A_0' = f[C_0' * C_1' * \cdots * C_{l-1}']$ is a subspace of A_0. A_0' is said to be a *linear subcode* of A_0. We can partition A_0 based on A_0' by first partitioning $C_0 * C_1 * \cdots * C_{l-1}$ based on the subcode $C_0' * C_1' * \cdots * C_{l-1}'$ and then performing bits-to-signal mapping based on $f(\cdot)$. Let k_0' be the dimension of A_0'. Then, the partition A_0/A_0' consists of $2^{k-k_0'}$ cosets (or cospaces) of A_0'.

Now, we are ready to construct q inner codes for a q-level CCM system. First, we form q linear subcodes of A_0, denoted by $A_1, A_2, \cdots, A_q$, such that the following conditions are met:

1. $A_0 \supset A_1 \supset \cdots \supset A_q$.
2. $A_q = \{f(\mathbb{0})\}$, where $\mathbb{0}$ is the all-zero codeword in $C_0 * C_1 * \cdots * C_{l-1}$.
3. For $0 < i \le q$, let k_i be the dimension of A_i. Then,

$$k_i = k_{i-1} - m_i. \tag{19.33}$$

It follows from (19.32) and (19.33) that

$$\begin{aligned} k_1 &= m_2 + m_3 + \cdots + m_q, \\ k_2 &= m_3 + m_4 + \cdots + m_q, \\ &\vdots \\ k_{q-1} &= m_q, \\ k_q &= 0. \end{aligned} \tag{19.34}$$

For $0 \le i \le q$, let $d_i^2 \triangleq d_E^2[A_i]$ be the MSE distance of A_i. Then,

$$d_0^2 \le d_1^2 \le \cdots \le d_q^2.$$

We partition A_0 into 2^{m_1} cosets based on A_1 (or modulo-A_1). Let A_0/A_1 denote this partition. The MSE distance of each coset in A_1/A_0 is d_1^2. A_0/A_1 is called the *coset code* of A_0 modulo-A_1. Next, we partition each coset in A_0/A_1 into 2^{m_2} cosets based on A_2. Let $A_0/A_1/A_2$ denote this second-level partition of A_0. Then, $A_0/A_1/A_2$ consists of $2^{m_1+m_2}$ cosets of A_2 in A_0. The MSE distance of each coset in $A_0/A_1/A_2$ is d_2^2. $A_0/A_1/A_2$ is called the coset code of A_0/A_1 modulo-A_2. We continue this partition process to form coset codes. For $1 \le i \le q$, let $A_0/A_1/\cdots/A_{i-1}$ be the coset code of $A_0/A_1/\cdots/A_{i-2}$ modulo-A_{i-1}. We partition each coset in $A_0/A_1/\cdots/A_{i-1}$ into 2^{m_i} cosets based on A_i. Then, $A_0/A_1/\cdots/A_i$ is the coset code of $A_0/A_1/\cdots/A_{i-1}$ modulo-A_i. The MSE distance of a coset in $A_0/A_1/\cdots/A_i$ is d_i^2. Each coset in $A_0/A_1/\cdots/A_q$ consists of only one codeword in

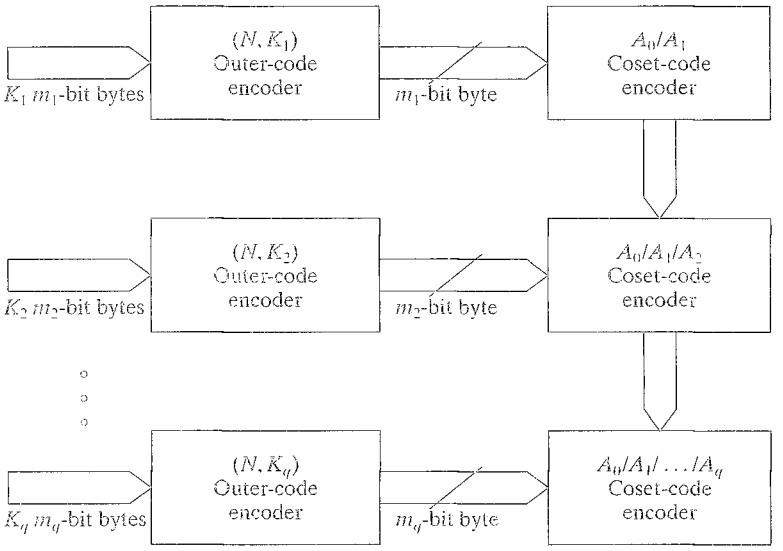

FIGURE 19.17: An overall multilevel concatenation encoder.

A_0, and $d_q^2 = \infty$. The foregoing partition process results in a sequence of q coset codes,

$$A_0/A_1,$$
$$A_0/A_1/A_2,$$
$$\vdots$$
$$A_0/A_1/\cdots/A_q.$$

These q coset codes are used as inner codes in a q-level CCM system. An organization of the overall encoder for a q-level CCM system is shown in Figure 19.17. Every inner encoder, except for the first level, has two inputs, one from the output of the outer-code encoder, and one from the output of the inner-code encoder of the preceding level.

For $1 \le i \le q$, the input of ith inner encoder from the output of the $(i-1)$th inner encoder is a sequence of cosets from the coset code $A_0/A_1/\ldots/A_{i-1}$. The ith-level is encoded in two steps:

1. *Outer-code encoding* A message of K_i m_i-bit bytes is encoded into a codeword of N m_i-bit bytes in the ith-level outer code B_i.
2. *Inner-code encoding* The input coset from the output of the inner-code encoder of the preceding level is partitioned into 2^{m_i} cosets modulo-A_i. Each m_i-bit-byte input from the ith-level outer code encoder is encoded into a coset in the partition $A_0/A_1/\ldots/A_i$. Therefore, the output of the ith-level inner-code encoder is a sequence of cosets from $A_0/A_1/\ldots/A_i$.

The output of the qth inner-code encoder is a sequence of codewords from the base code A_0. It is a sequence of Nn signals from the signal space S. The overall q-level CCM system generates a concatenated modulation code $\tilde{C}$ of length Nn, dimension

$$\tilde{K} = m_1 K_1 + m_2 K_2 + \cdots + m_q K_q,$$

and MSE distance

$$d_E^2[\tilde{C}] \geq \min_{1 \leq i \leq q} \{D_i d_{i-1}^2\} \tag{19.35}$$

(see Problem 19.3). The spectral efficiency of $\tilde{C}$ is

$$\eta[\tilde{C}] = \frac{\tilde{K}}{Nn} \text{ bits/symbol.}$$

Multistage decoding of a multilevel concatenated modulation code is similar to the multistage decoding of a multilevel BCM code presented in the previous section. Let $\mathbb{V} = (\mathbb{v}_0, \mathbb{v}_1, \ldots, \mathbb{v}_{N-1})$ be a codeword in $\tilde{C}$, where for $0 \leq j < N$, $\mathbb{v}_j$ is a codeword in the base inner code A_0. Each $\mathbb{v}_j$ must be in one of the cosets of the coset code A_0/A_1. Let $\mathbb{R} = (\mathbb{r}_0, \mathbb{r}_1, \ldots, \mathbb{r}_{N-1})$ be the received sequence. $\mathbb{R}$ is decoded in q steps, from the first level to the qth level, as shown in Figure 19.18. At the first level of decoding, $\mathbb{r}_j$ is decoded into one of the cosets in A_0/A_1. Based

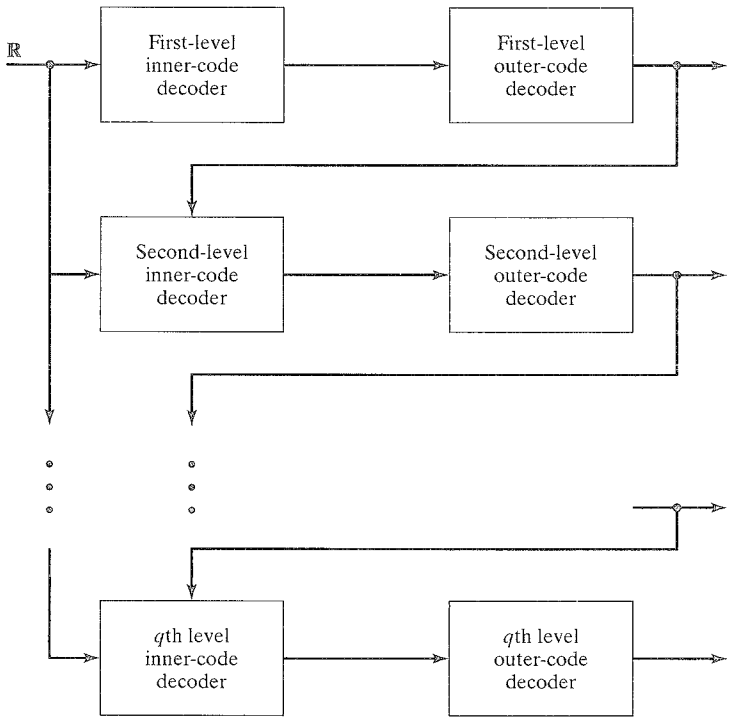

FIGURE 19.18: A decoder for a q-level concatenated modulation code.

on the decoded coset, the m_1-bit byte $\mathbb{a}_j^{(1)}$ is identified that is the estimate of the output byte of the first-level outer-code B_1 encoder at time-j. Then, the sequence $(\mathbb{a}_0^{(1)}, \mathbb{a}_1^{(1)}, \ldots, \mathbb{a}_{N-1}^{(1)})$ is decoded based on the outer code B_1. Let $(b_0^{(1)}, b_1^{(1)}, \ldots, b_{N-1}^{(1)})$ be the decoded codeword. Then, the estimated message sequence is retrieved from this decoded codeword. Furthermore, from this decoded codeword, a coset sequence

$$(\Omega_0^{(1)}, \Omega_1^{(1)}, \ldots, \Omega_{N-1}^{(1)})$$

is reproduced at the output of the first-level decoder, where $\Omega_j^{(1)} \in A_0/A_1$. This coset sequence is then applied at the input of the second-level decoder.

Now, the second-level decoding begins. For $0 \leq j < N$, based on the input information $\Omega_j^{(1)}$, we decode $\mathbb{r}_j$ into one of the cosets in $\Omega_j^{(1)}/A_2$. Based on the decoded coset, the corresponding m_2-bit byte $\mathbb{a}_j^{(2)}$ is identified that is the estimate of the output byte of the second-level outer-code B_2 encoder at time-j. The sequence $(\mathbb{a}_0^{(2)}, \mathbb{a}_1^{(2)}, \ldots, \mathbb{a}_{N-1}^{(2)})$ is decoded into a codeword $(b_0^{(2)}, b_1^{(2)}, \ldots, b_{N-1}^{(2)})$ in the second-level outer code B_2. Based on $(b_0^{(2)}, b_1^{(2)}, \ldots, b_{N-1}^{(2)})$, a coset sequence

$$(\Omega_0^{(2)}, \Omega_1^{(2)}, \ldots, \Omega_{N-1}^{(2)})$$

is reproduced at the output of the second-level decoder, where $\Omega_j^{(2)} \in A_0/A_1/A_2$. This coset sequence is then applied at the input of the third-level decoder. Other levels of decoding are carried out in the same manner.

To keep decoding complexity low while maintain good error performance, the inner codes are decoded with a soft-decision decoding algorithm, and the outer codes are decoded algebraically.

EXAMPLE 19.7

This example gives a two-level CCM system with $m_1 = m_2 = 8$. The first-level outer code B_1 is the NASA standard (255, 223) RS code over $GF(2^8)$, and the second-level outer code B_2 is the (255, 239) RS code over $GF(2^8)$. The base modulation inner code A_0 is the 3-level 8-PSK BCM code $f[C_0 * C_1 * C_2]$, where C_0 is the (8, 1) repetition code, C_1 is the (8, 7) SPC code, and C_2 is the (8, 8) universal code. The dimension of A_0 is $k_0 = 16$, and $d_E^2(A_0) = 4$. To construct a subspace A_1 of A_0 with dimension $k_1 = k_0 - m_1 = 8$, we choose the following three binary component codes: (1) $C_0^{(1)} = (8, 0)$ is the code of length 8 consisting of only the all-zero sequence, (2) $C_1^{(1)} = (8, 1)$ is the repetition code of length 8, (3) $C_2^{(1)} = (8, 7)$ is the SPC code of length 8. Let $A_1 = f[C_0^{(1)} * C_1^{(1)} * C_2^{(1)}]$. The dimension of A_1 is $k_1 = 8$. Because $C_0^{(1)} \subset C_0$, $C_1^{(1)} \subset C_1$, $C_2^{(1)} \subset C_2$, A_1 is a subspace of A_0. From (19.7) the MSE distance of A_1 is $d_1^2 = d_E^2[A_1] = 8$. The coset code A_0/A_1 consists of 2^8 cosets modulo-A_1.

Let $A_2 = \{f(\mathbb{0})\}$. Then, the coset code $A_0/A_1/A_2$ consists of 2^{16} cosets modulo-A_2. Each coset consists of only one codeword in A_0. The overall encoder for the 2-level CCM system is shown in Figure 19.19. The 2-level concatenated modulation

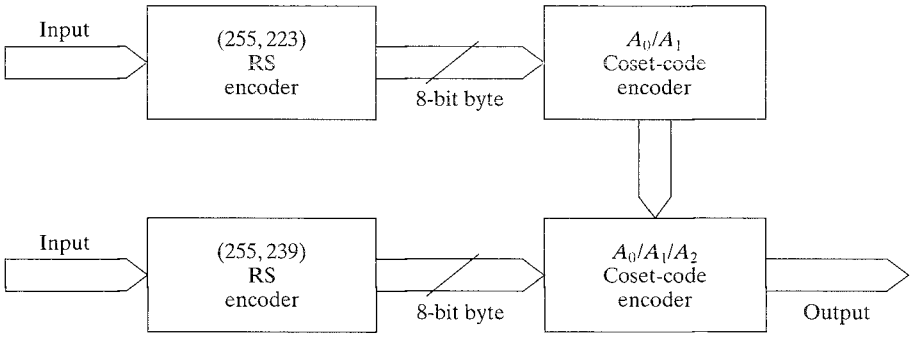

FIGURE 19.19: An encoder for a 2-level concatenated coded modulation system.

code $\tilde{C}_i$ has length 2040, dimension 3696, and MSE distance $d_E^2[\tilde{C}] = 132$. The spectral efficiency is

$$\eta[\tilde{C}] = \frac{3696}{2040} = 1.818 \text{ bits/symbol}.$$

A_0 has a 4-state 8-section trellis, as shown in Figure 19.6. A_1 also has a 4-state 8-section trellis but without parallel branches between two adjacent states (see Problem 19.3). Soft-decision decodings of inner codes are relatively simple. The error performance of this 2-level CCM system is shown in Figure 19.20. It achieves a 5.3-dB real coding gain over uncoded QPSK at a BER of 10^{-6}. This 2-level CCM system has higher spectral efficiency and better error performance than the single-level CCM system constructed in Example 19.6.

In general, a q-level CCM system can achieve higher spectral efficiency and better error performance than a single-level CCM system.

19.5 PRODUCT CODED MODULATION

Coded modulation also can be combined with the product coding technique to form product coded modulation [22] systems to achieve large coding gains with high spectral efficiencies.

Let S be a signal space with 2^l signal points. Each signal point $s \in S$ is labeled with a binary string of l bits, $a^{(0)}a^{(1)} \ldots a^{(l-1)}$, through a binary partition chain. Let $f(\cdot)$ be the bits-to-signal mapping defined by the binary partition of S, for which $f(a^{(0)}a^{(1)} \ldots a^{(l-1)}) = s$.

For $0 \leq i < l$, let $P_i = C_{i,1} \times C_{i,2}$ be a two-dimensional product code, where

1. $C_{i,1}$ is the row code and is an $(N, k_{i,1}, d_{i,1})$ linear block code.
2. $C_{i,2}$ is the column code and is an $(n, k_{i,2}, d_{i,2})$ linear block code.

Let $\mathcal{A}^{(0)}, \mathcal{A}^{(1)}, \ldots, \mathcal{A}^{(l-1)}$ be l two-dimensional code arrays in the product codes $P_0, P_1, \ldots, P_{l-1}$, respectively. For $0 \leq q < l$, $0 \leq i < n$, and $0 \leq j < N$, let $a_{i,j}^{(q)}$ be the code bit at the ith row and jth column of the qth code array $\mathcal{A}^{(q)}$. We form the

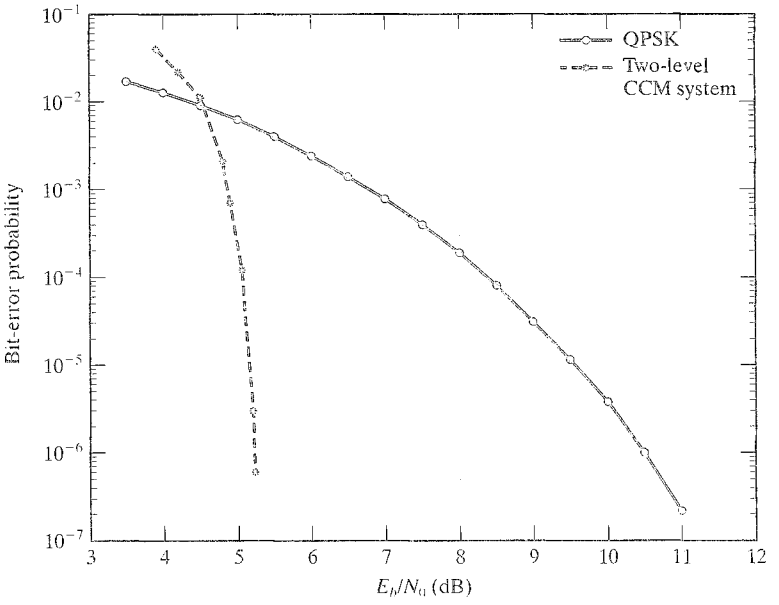

FIGURE 19.20: Bit-error performance of the two-level CCM system given in Example 19.7.

following $n \times N$ signal array over S:

$$\begin{aligned} \mathcal{A}_s &\triangleq f(\mathcal{A}^{(0)} * \mathcal{A}^{(1)} * \cdots * \mathcal{A}^{(l-1)}) \\ &= [f(a_{i,j}^{(0)} a_{i,j}^{(1)} \ldots a_{i,j}^{(l-1)})]_{0 \le i < n,\ 0 \le j < N} . \end{aligned} \tag{19.36}$$

Each row of $\mathcal{A}_s$ is a codeword in the l-level BCM code $\Phi_0 \triangleq f[C_{0,1} * C_{1,1} * \ldots * C_{l-1,1}]$ over S, and each column of $\mathcal{A}_s$ is a codeword in the l-level BCM code $\Phi_1 \triangleq f[C_{0,2} * C_{1,2} * \ldots * C_{l-1,2}]$ over S. Therefore, the following collection of signal arrays

$$\begin{aligned} \Phi_p &\triangleq f[P_0 * P_1 * \ldots * P_{l-1}] \\ &= \{f(\mathcal{A}^{(0)} * \mathcal{A}^{(1)} * \ldots * \mathcal{A}^{(l-1)}) : \mathcal{A}^{(q)} \in P_q \text{ with } 0 \le q < l\} \end{aligned} \tag{19.37}$$

is the product of Φ_0 and Φ_1, which are called the row and column component codes of Φ_p. Φ_p is an l-level product BCM code with length Nn and dimension $k_{0,1} \times k_{0,2} + k_{1,1} \times k_{1,2} + \cdots + k_{l-1,1} \times k_{l-1,2}$. The spectral efficiency of Φ_p is

$$\eta[\Phi_p] = \frac{\sum_{i=0}^{l-1} k_{i,1} \times k_{i,2}}{Nn} \text{ bits/symbol}$$

and the MSE distance of Φ_p is

$$d_E^2[\Phi_p] = \sum_{i=0}^{l-1} d_{i,1} \times d_{i,2} \times \Delta_i^2,$$

where Δ_i^2 is the intraset distance of the ith level of the binary partition of the signal space S.

A signal array $\mathcal{A}_s$ in Φ_p consists of l layers of binary code arrays. Each layer contributes a labeling bit in the bits-to-signal mapping. Multistage decoding of Φ_p can be carried out layer by layer. Decoding a layer consists of two steps. At the first step, the columns (or rows) are decoded with soft-decision multistage decoding based on the column (or row) code Φ_1 (or Φ_0). After column (or row) decoding, the rows (or columns) are decoded algebraically based on the binary row code $C_{i,1}$ (or the binary column code $C_{i,2}$). At the end of row (or column) decoding, a decoded array is obtained. This decoded array is then passed down for decoding the next layer. This process continues until the last layer is decoded. A layer is decoded with a combination of soft- and hard-decision decoding to decrease decoding complexity. Other decoding arrangements are possible. For example, columns and rows of a layer can be decoded separately based on column code Φ_1 and row code Φ_0, respectively, using multistage soft-decision decoding. The two decodings are compared, and the mismatches are declared erasures. Erasure decoding [23] is then performed to correct the erasures. This completes the layer decoding. Decoding this way improves the error performance but also increases decoding complexity.

EXAMPLE 19.8

This example demonstrates the construction of a 3-level 8-PSK product code. The three binary row codes are $C_{0,1} = (1023, 648)$, $C_{1,1} = (1023, 893)$, and $C_{2,1} = (1023, 1003)$ BCH codes with minimum designed distances 83, 27, and 5, respectively. The three binary column codes are as follows: (1) $C_{0,2}$ is the (16, 5) RM code of minimum distance 8; (2) $C_{1,2}$ is the (16, 15) even-parity-check code; and (3) $C_{2,2}$ is the (16, 16) universal code. The resultant 3-level 8-PSK product code Φ_p has a spectral efficiency of 1.9968 bits/symbol. In multistage decoding, the column code $\Phi_1 = f[(16, 5) * (16, 15) * (16, 16)]$ is decoded with multistage soft-decision decoding. The row code of each layer is decoded algebraically. The (16, 5) RM code has an 8-state 4-section trellis, and the (16, 15) SPC code has a 2-state trellis. Therefore, trellis-based 3-stage decoding of the column code Φ_1 is relatively simple. The product modulation code Φ_p achieves a 5-dB real coding gain over the uncoded QPSK system at BER $= 10^{-6}$ and a 6.1-dB coding gain at BER $= 10^{-9}$ [22].

19.6 MULTILEVEL CODED MODULATION FOR UNEQUAL ERROR PROTECTION

In certain communication systems an information sequence may consist of several parts that have different degrees of significance and hence require different levels of protection against noise. Codes that are designed to provide different levels of data protection are known as *unequal error protection* (UEP) codes. UEP codes were first studied by Masnick and Wolf [24] and later by many others. Multilevel BCM codes with multistage decoding are quite suitable for unequal error protection. When such a code is used, different code levels provide different degrees of protection for different parts of a transmitted information sequence.

Let $\mathbb{m} = (\mathbb{m}_0, \mathbb{m}_1, \ldots, \mathbb{m}_{l-1})$ be a message of k bits, where for $0 \leq i < l$, $\mathbb{m}_i$ is the ith part of the message and consists of k_i information bits. Suppose $\mathbb{m}_0$ is

the most significant part of the message $\mathbf{m}$, and $\mathbf{m}_{l-1}$ is the least significant part of $\mathbf{m}$. Hence, $\mathbf{m}_0$ requires more protection against errors than the other parts, and $\mathbf{m}_{l-1}$ requires the least protection. For $0 \leq i < l$, let C_i be an (n, k_i, d_i) binary linear block code of length n, dimension k_i, and minimum Hamming distance d_i. Consider the l-level BCM code $f[C_0 * C_1 * \ldots * C_{l-1}]$ over a signal space S. Suppose a message $\mathbf{m} = (\mathbf{m}_0, \mathbf{m}_1, \ldots, \mathbf{m}_{l-1})$ is to be encoded into a signal sequence in $f[C_0 * C_1 * \ldots * C_{l-1}]$. First, the ith part $\mathbf{m}_i$ is encoded into a codeword $\mathbf{v}_i$ in C_i. Then, the interleaved sequence $\mathbf{v}_0 * \mathbf{v}_1 * \ldots * \mathbf{v}_{l-1}$ is mapped into a signal sequence $f(\mathbf{v}_0 * \mathbf{v}_1 * \ldots * \mathbf{v}_{l-1})$ in the l-level BCM code $f[C_0 * C_1 * \ldots * C_{l-1}]$. This signal sequence is the codeword for the message $\mathbf{m}$. For simplicity, we use $f(\mathbf{m})$ to denote this codeword. Let $\mathbf{m}' = (\mathbf{m}'_0, \mathbf{m}'_1, \ldots, \mathbf{m}'_{l-1})$ be another message such that for $0 \leq i < l$, $\mathbf{m}'_i \neq \mathbf{m}_i$, and $\mathbf{m}'_j = \mathbf{m}_j$ with $j < i$. It follows from the proof of Theorem 19.1 that

$$d_E^2(f(\mathbf{m}), f(\mathbf{m}')) \geq d_i \Delta_i^2.$$

In fact,

$$d_i \Delta_i^2 = \min\{d_E^2(f(\mathbf{m}), f(\mathbf{m}')) : \mathbf{m}'_i \neq \mathbf{m}_i, \text{ and } \mathbf{m}'_j = \mathbf{m}_j \text{ for } j < i\}. \quad (19.38)$$

This simply says that if two messages are identical in the first $i-1$ parts but different in the ith part, then their corresponding codewords are separated by a squared Euclidean distance of at least $d_i \Delta_i^2$. This implies that the ith part of a message is protected by the SE distance $d_i \Delta_i^2$. Therefore, for an l-level BCM code to provide unequal error protection for various parts of a message, the following condition on distances,

$$d_0 \Delta_0^2 \geq d_1 \Delta_1^2 \geq \ldots \geq d_{l-1} \Delta_{l-1}^2, \quad (19.39)$$

must hold.

So far, the construction of TCM and BCM codes presented here and in previous chapters is based on the conventional Ungerboeck symmetrical binary partition of a conventional symmetrical signal space S, either an MPSK or a QAM signal constellation. This conventional signal set partitioning for maximizing intraset distance at each level is good for constructing modulation codes for one-level error protection; however, multilevel BCM codes constructed based on this conventional signal set partitioning and the distance condition of (19.39) do not perform well for unequal error protection with multistage decoding, especially for small-to-medium SNRs, owing to the large increase in effective error coefficients in the first several decoding stages. Let $A_{d_0}^{(0)}$ denote the number of nearest neighbors of a codeword in C_0. With multistage decoding, the error coefficient at the first decoding stage becomes $2^{d_0} \cdot A_{d_0}^{(0)}$ rather than $A_{d_0}^{(0)}$. For large d_0, $2^{d_0} \cdot A_{d_0}^{(0)}$ becomes very large. For small-to-medium SNRs, the error performance is mainly determined by the error coefficient. This large increase in error coefficient degrades the error performance at the first several stages of decoding so much that it destroys the unequal error protection capability for which the code is designed. The most significant part, $\mathbf{m}_0$, of a message is no longer well protected. The poor performance of the first stage of decoding propagates to the subsequent stages and results in poor overall

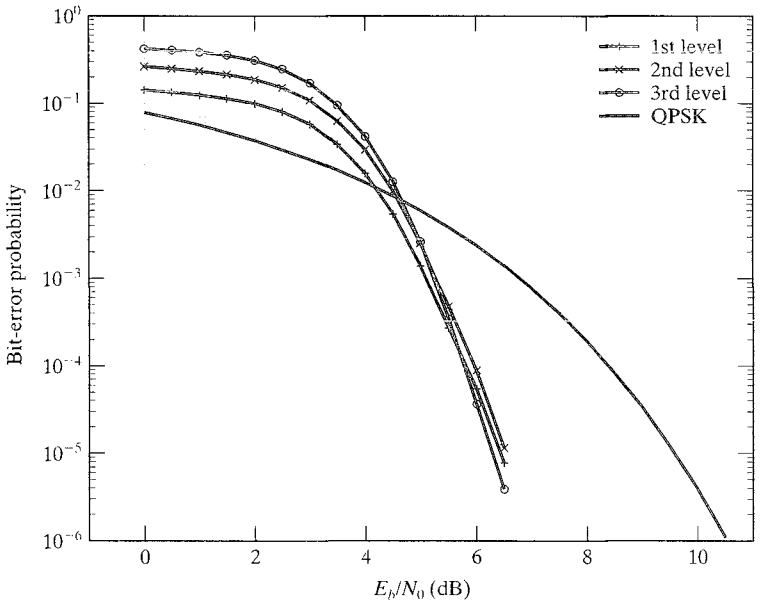

FIGURE 19.21: Bit-error performances of various levels of a 3-level 8-PSK BCM code for unequal error protection with Ungerboeck's signal partition.

performance in terms of unequal error protection. Figure 19.21 shows the error performances at various levels of a 3-level 8-PSK BCM code with (64, 18, 22), (64, 57, 4), and (64, 63, 2) extended BCH codes as binary component codes. The MSE distances at three levels are $d_0 \cdot \Delta_0^2 = 22 \times 0.586 = 12.892$, $d_1 \cdot \Delta_1^2 = 4 \times 2 = 8$, and $d_2 \cdot \Delta_2^2 = 2 \times 4 = 8$, respectively. The spectral efficiency of the code is $\eta[C] = 2.156$ bits/symbol. From Figure 19.21 we see that for large SNR this code does provide two levels of error protection; however, for small-to-medium SNRs, the increase in error coefficient by a factor of 2^{22} at the first decoding stage totally destroys the unequal error protection capability, and all three levels perform poorly; in fact, the first level, with larger MSE distance, performs even worse than the other two levels. For BERs greater than 10^{-5}, there is no unequal error protection.

Several approaches have been proposed [25–28] for designing good multilevel BCM codes to provide distinct unequal error protection for various levels. These approaches use either nonconventional signal set partition or nonconventional signal constellations or both. In this section we present a nonconventional signal set partition of conventional signal constellations for designing multilevel BCM codes for unequal error protection. The approach is to reduce the error coefficient and to prevent or minimize error propagation from the first stage of decoding. Special examples with different signal spaces are used to explain the signal set partitioning, code construction, and multistage decoding.

Consider the conventional 8-PSK signal space. We partition this signal space and label its signal points as shown in Figure 19.22. At the first level, the signal set is partitioned into two subsets of equal size, denoted by $Q(0)$ and $Q(1)$; the four

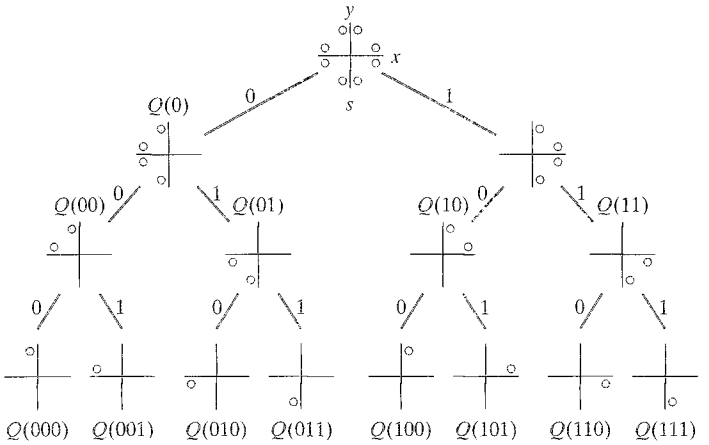

FIGURE 19.22: Block partition of the 8-PSK constellation.

signal points of $Q(0)$ lie in the left-half plane with first labeling bit $a_0 = 0$, and the four signal points of $Q(1)$ lie in the right-half plane with first labeling bit $a_0 = 1$. At the second level of partition, $Q(0)$ is partitioned into two subsets, denoted by $Q(00)$ and $Q(01)$; the two signal points in $Q(00)$ lie in the upper quadrant of the left-half plane with second labeling bit $a_1 = 0$, and the two signal points in $Q(01)$ lie in the lower quadrant of the left-half plane with second labeling bit $a_1 = 1$. $Q(1)$ is also partitioned into two subsets of equal size, denoted by $Q(10)$ and $Q(11)$; the two signal points of $Q(10)$ lie in the upper quadrant of the right-half plane with second labeling bit $a_1 = 0$, and the two signal points of $Q(11)$ lie in the lower quadrant of the right-half plane with second labeling bit $a_1 = 1$. Finally, each subset at the second level is partitioned into two subsets, each with only one signal point with the third labeling bit $a_2 = 0$ or 1. Let (x, y) denote the coordinates of an 8-PSK signal point in the real plane R^2. The labeling has the following properties:

1. $x > 0$ for all the signal points with first labeling bit $a_0 = 1$, and $x < 0$ for all the signal points with first labeling bit $a_0 = 0$.
2. $y > 0$ for all the signal points with the second labeling bit $a_1 = 0$, and $y < 0$ for all the signal points with second labeling bit $a_1 = 1$.
3. The third labeling bit a_2 specifies the point in the quadrant given by $a_0 a_1$.

Therefore, the first and second labeling bits of a signal point correspond to its x- and y-coordinates, respectively. With this labeling structure, the first and second stages of decoding can be carried out independently and simultaneously in parallel, as shown in Figure 19.23. This removes the error propagation from the first stage of decoding to the second stage and also reduces decoding delay; however, the foregoing partition does not have the monotonically increasing intraset distance property; in fact, the intraset distances at all three levels are equal: $\Delta_0^2 = \Delta_1^2 = \Delta_2^2 = 0.586$. For small-to-medium SNR, this loss of intraset distances of the second and third level is more than compensated for by the drastic reduction in error coefficients, as will be shown later.

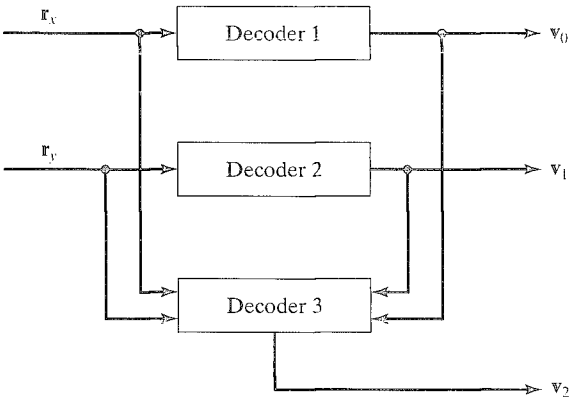

FIGURE 19.23: Decoder for 3-level coded 8-PSK modulation.

Let $\mathbb{r} = ((r_{x,0}, r_{y,0}), (r_{x,1}, r_{y,1}), \ldots, (r_{x,n-1}, r_{y,n-1}))$ be the two-dimensional received vector at the output of the matched filter, where (r_{xj}, r_{yj}) denotes the coordinates of the jth received signal. Let $\mathbb{r}_x \triangleq (r_{x,0}, r_{x,1}, \ldots, r_{x,n-1})$ and $\mathbb{r}_y \triangleq (r_{y,0}, r_{y,1}, \ldots, r_{y,n-1})$ denote the projections of $\mathbb{r}$ on the x- and y-axes, respectively, called the *in-phase* and *quadrature components* of $\mathbb{r}$. Then, the decoders at the first and second stages simply operate on $\mathbb{r}_x$ and $\mathbb{r}_y$, independently. Let $\mathbb{v}_0 = (v_{0,0}, v_{0,1}, \ldots, v_{0,n-1})$ and $\mathbb{v}_1 = (v_{1,0}, v_{1,1}, \ldots, v_{1,n-1})$ be the decoded codewords at the first and second stages. They are then passed to the third decoding stage for decoding the third component code C_2. The third stage of decoding is carried out as follows. First, we form a one-dimensional projection of $\mathbb{r} = (\mathbb{r}_x, \mathbb{r}_y)$,

$$\mathbb{r}' = (r'_0, r'_1, \ldots, r'_n),$$

where

$$r'_j = \begin{cases} -(r_{xj} - r_{yj}) & \text{for} \quad v_{0,j} = v_{1,j} = 0, \\ -(r_{xj} + r_{yj}) & \text{for} \quad v_{0,j} = 0 \text{ and } v_{1,j} = 1, \\ (r_{xj} - r_{yj}) & \text{for} \quad v_{0,j} = v_{1,j} = 1, \\ (r_{xj} + r_{yj}) & \text{for} \quad v_{0,j} = 1 \text{ and } v_{1,j} = 0. \end{cases} \tag{19.40}$$

Analysis shows that for $i = 0$ and 1, the bit-error probability of the ith stage of decoding is upper bounded as follows [27]:

$$P_{bi} \leq \sum_{\omega=d_i}^{n} \frac{\omega A_\omega^{(i)} 2^{-\omega}}{n} \sum_{j=0}^{\omega} \binom{n}{\omega} Q\left(\sqrt{d_p^2(j)}\right), \tag{19.41}$$

where

1. $A_\omega^{(i)}$ is the number of codewords in C_i with weight ω,
2. $$d_p^2(j) = \frac{1}{\omega}(j\xi_1 + (\omega - j)\xi_2)^2. \tag{19.42}$$

3.
$$\xi_1 = \sin(\pi/8) \text{ and } \xi_2 = \cos(\pi/8), \tag{19.43}$$

4.
$$Q(x) \triangleq \frac{1}{\sqrt{\pi N_0}} \int_{x\sqrt{\eta E_b}}^{\infty} e^{-\tau^2/N_0} d\tau \tag{19.44}$$

(η is the spectral efficiency of the 3-level 8-PSK BCM code).

The bit-error probability of the third-stage decoding is upper bounded by

$$P_{b2} \leq \sum_{\omega=d_2}^{n} \frac{\omega A_\omega^{(2)}}{n} Q\left(\sqrt{\omega \xi_1^2}\right). \tag{19.45}$$

If the Ungerboeck partitioning is used for labeling signal points, the bit-error probability of first-stage decoding is upper bounded by

$$P_{b1}^{(UG)} \leq \sum_{\omega=d_0}^{n} \frac{\omega}{n} A_\omega^{(0)} 2^\omega Q\left(\sqrt{\omega \xi_1^2}\right). \tag{19.46}$$

The bound of (19.41) shows that the nonconventional signal set partition shown in Figure 19.22 results in an error coefficient of $2^{-d_0} A_{d_0}^{(0)}$ at the first-stage decoding; however, the conventional Ungerboeck signal set partition results in an error coefficient of $2^{d_0} A_{d_0}^{(0)}$ at the first-stage decoding, as shown in (19.46). Thus, there is a factor of 2^{2d_0} reduction in error coefficient. This reduction in error coefficient results in a significant coding gain for small-to-medium SNR that more than compensates for the intraset distance loss.

Consider the 3-level 8-PSK BCM code $f[C_0 * C_1 * C_2]$ in which the binary component codes are (64, 18, 22), (64, 45, 8), and (64, 63, 2) extended BCH codes. This BCM code has spectral efficiency $\eta[C]$ of almost 2 bits/symbol and SE distances $d_0\Delta_0^2 = 12.892$, $d_1\Delta_1^2 = 4.688$, and $d_2\Delta_2^2 = 1.172$ at three levels. Bit-error performances at three levels and their corresponding upper bounds of this code are given in Figure 19.24, which shows that the code possesses three distinct levels of error protection, even for very low SNR. At BER $= 10^{-5}$, an 8.8-dB coding gain over the uncoded QPSK is attained at the first decoding level, whereas the corresponding asymptotic coding gain is only $10\log_{00}(12.892/2) = 8.02$ dB.

The foregoing nonconventional signal set partitioning is called *block partitioning*. This partitioning technique can be applied to partition a QAM signal space and label its signal points. Block partitions of the 16-QAM and 64-QAM are shown in Figures 19.25 and 19.26, respectively. Let (x, y) be the coordinates of a signal point. Again, the signal labeling has the following polarity property:

1. $x > 0$ for all the signal points with first labeling bit $a_0 = 1$, and $x < 0$ for all the signal points with first labeling bit $a_0 = 0$.
2. $y > 0$ for all the signal points with second labeling bit $a_1 = 0$, and $y < 0$ for all the signal points with second labeling bit $a_1 = 1$.

If a 6-level 64-QAM BCM code is constructed based on the preceding block partitioning and signal labeling, the first and second stages of decoding can be

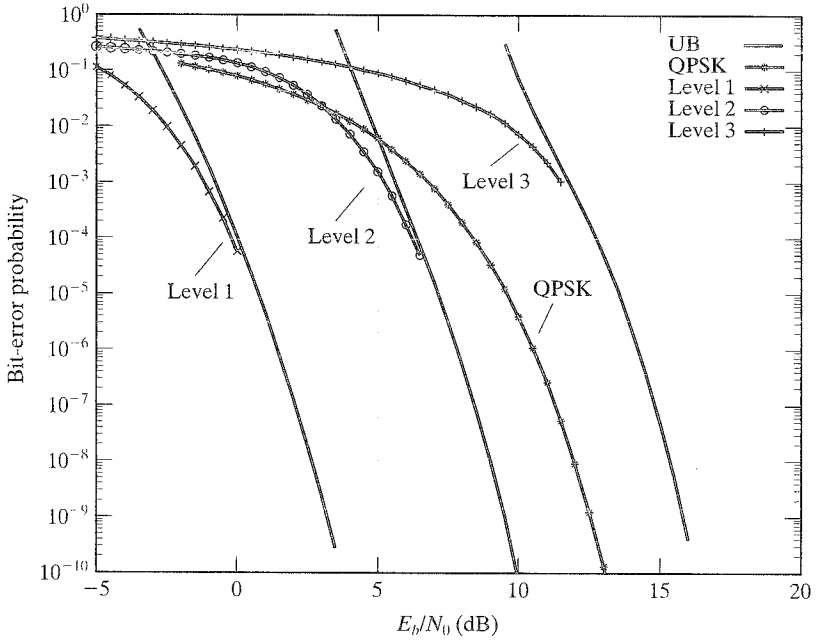

FIGURE 19.24: Bit-error performances of various levels of an unequal error protection 3-level 8-PSK BCM code with block signal set partition.

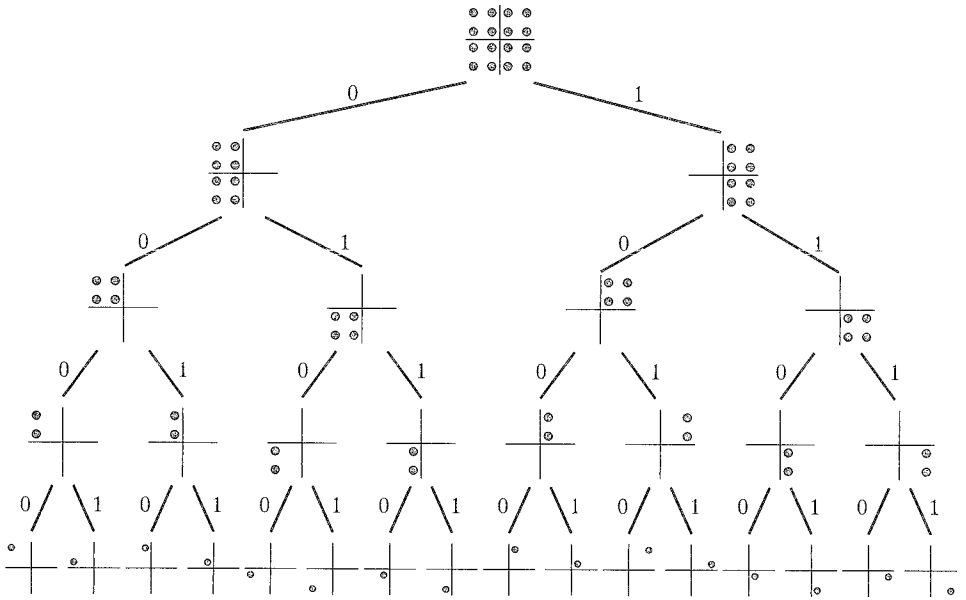

FIGURE 19.25: Block partition of a 16-QAM.

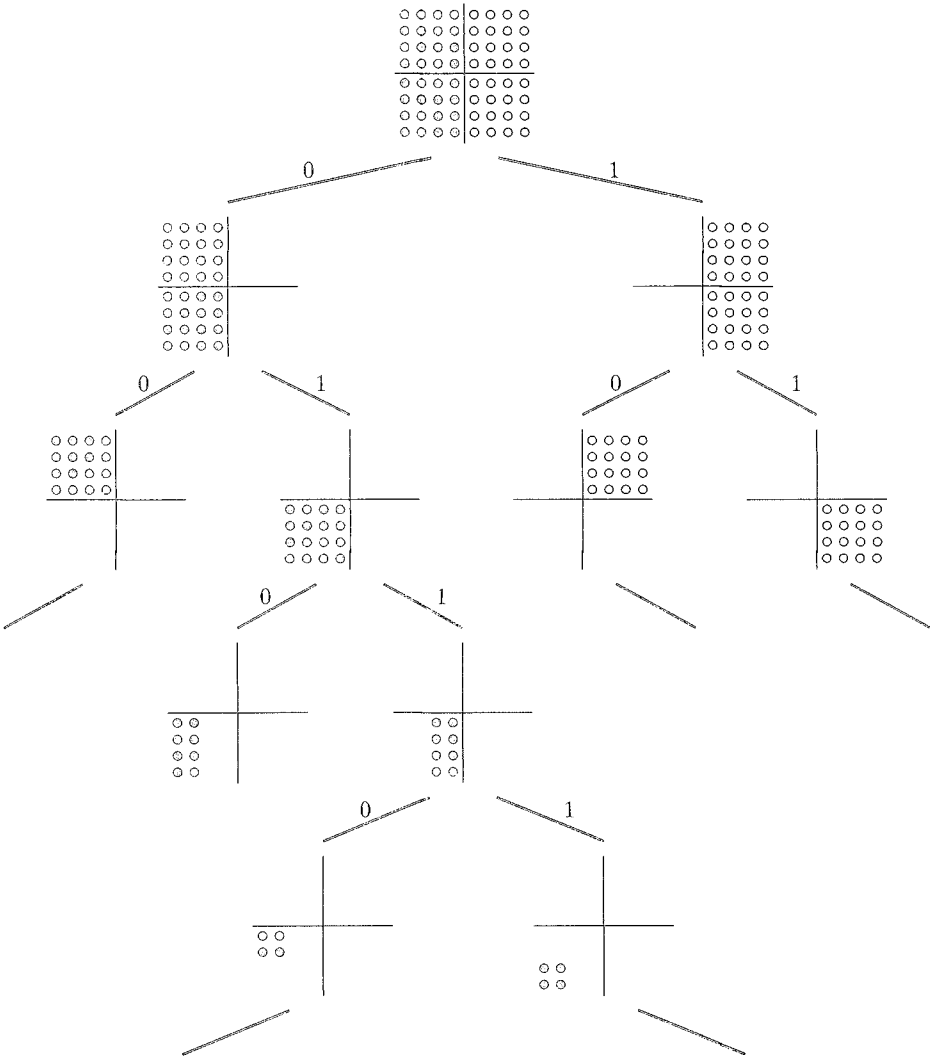

FIGURE 19.26: Block partition of a 64-QAM.

carried out independently. For $i = 0$ and 1, the bit-error probabilities of the first and second stages of decoding are the same and are upper bounded by

$$P_{bi} \leq \sum_{\omega=d_i}^{n} \frac{\omega}{n} A_{\omega}^{(i)} 4^{-\omega} \sum_{i_1=0}^{\omega} \sum_{i_2=0}^{\omega-i_1} \sum_{i_3=0}^{\omega-i_1-i_2} \binom{\omega}{i_1} \binom{\omega - i_1}{i_2} \binom{\omega - i_1 - i_2}{i_3} Q\left(\sqrt{d_p^2(i_1, i_2, i_3)}\right), \tag{19.47}$$

where $d_p^2(i_1, i_2, i_3) = \frac{1}{\omega}[i_1\xi_1 + i_2\xi_2 + i_3\xi_3 + (\omega - i_1 - i_2 - i_3)\xi_4]^2$, and $\xi_1 = 1/\sqrt{42}$, $\xi_2 = 3\xi_1$, $\xi_3 = 5\xi_1$, and $\xi_4 = 7\xi_1$.

If we assume correct decoding at the first and second decoding stages, the bit-error probabilities of the third and fourth decoding stages are upper bounded as follows: For $i = 2$ and 3,

$$P_{bi} \leq \sum_{\omega=d_i}^{n} \frac{\omega}{n} A_{\omega}^{(i)} 2^{-\omega} \sum_{j=0}^{\omega} \binom{\omega}{j} Q(\sqrt{d_p^2(j)}), \tag{19.48}$$

where

$$d_p^2(j) = \frac{1}{\omega}[j\xi_1 + (\omega - j)\xi_2]^2.$$

If we assume that all the previous decodings are correct, the bit-error probabilities of the fifth and sixth decoding stages are upper bounded by

$$P_{bi} \leq \sum_{\omega=d_i}^{n} \frac{\omega}{n} A_{\omega}^{(i)} Q(\sqrt{\omega \xi_1^2}), \qquad \text{for } i = 4 \text{ and } 5. \tag{19.49}$$

Figure 19.27 shows the bit-error performance of a 6-level 64-QAM BCM code whose binary component codes are (64, 24, 16), (64, 24, 16), (64, 45, 8),(64, 51, 6), (64, 57, 4) and (64, 57, 4) extended BCH codes. This 6-level 64-QAM code provides four levels of error protection. The first and second levels have the same degree of error protection. These two levels consist of 48 information bits. The fifth and sixth

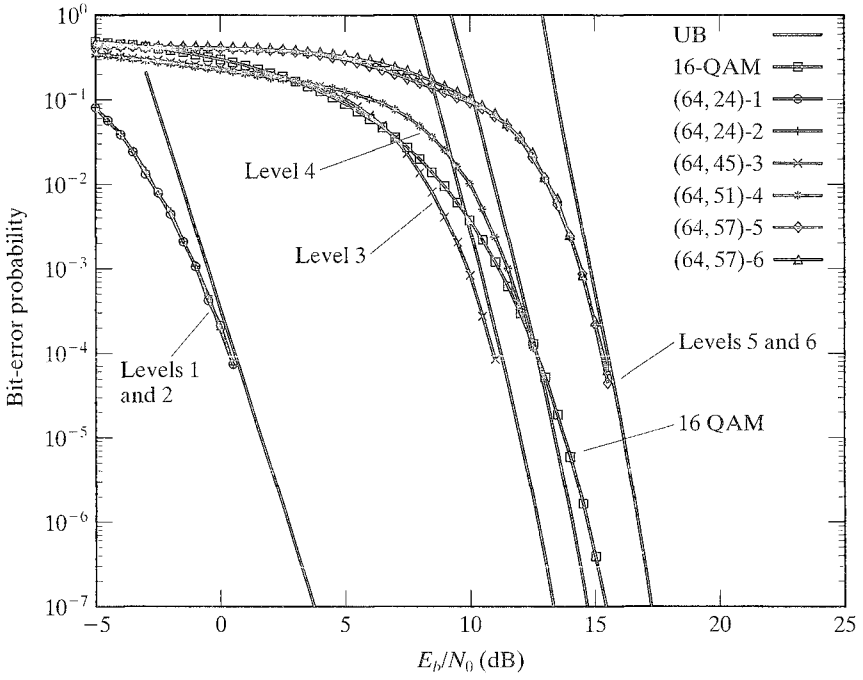

FIGURE 19.27: Bit-error performance of various levels of a 6-level 64-QAM BCM code for unequal error protection with block signal set partition.

levels also have the same degree of error protection. The spectral efficiency of the code is 4.013125 bits/symbol. At a BER of 10^{-5}, the first two levels achieve a 12-dB coding gain over the uncoded 16-QAM.

The disadvantage of block partitioning of a signal set is that the intraset distance at each partition level is the same. As a result, the error performance at the lower decoding levels may be poor. For example, Figure 19.24 shows that the third-level decoding results in an error performance worse than that of the uncoded QPSK. To overcome this problem, hybrid partitioning of a signal set can be used. Block partitioning is used at the first several partition levels, say the first and second levels, to provide independent decodings and to reduce error coefficients for minimizing the error propagation effect. Then, the conventional Ungerboeck partitioning is used for the remaining partition levels to increase intraset distances for improving the error performance of the lower decoding levels.

Figure 19.28 depicts a hybrid partition of the 8-PSK signal space. The first-level partition is block partition. The other two levels are Ungerboeck's partition. This hybrid partition results in intraset distances $\Delta_0^2 = \Delta_1^2 = 0.586$ and $\Delta_2^2 = 2$. Consider the 3-level 8-PSK BCM code given earlier in this section constructed by using the block signal set partitioning as shown in Figure 19.22. Suppose the same three binary component codes are used to construct a 3-level 8-PSK BCM code based on the hybrid partition shown in Figure 19.28. The MSE distances at three code levels are then $d_0\Delta_0^2 = 12.892$, $d_1\Delta_1^2 = 4.688$, and $d_2\Delta_2^2 = 4$. The MSE distance of the third code level is increased from 1.172 to 4. The bit-error performances of this code at three levels are shown in Figure 19.29. Compared with Figure 19.24, we see that the hybrid partition results in 4.4-dB coding gain at the third level at a BER of 10^{-5} but a loss of 2.3-dB coding gain at the second level. This is a good trade-off if the second part of a message is not much more significant than the third part of the message.

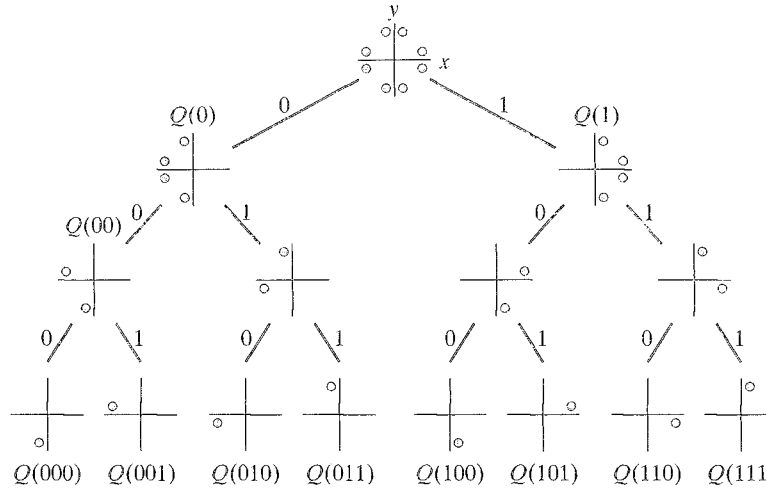

FIGURE 19.28: Hybrid partition of the 8-PSK constellation.

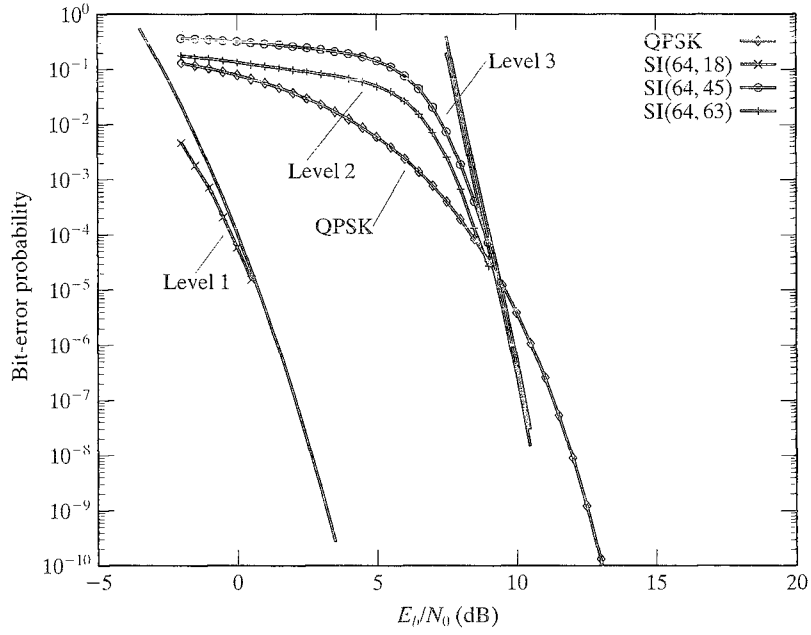

FIGURE 19.29: Bit-error performance of various levels of a 3-level 8-PSK BCM code for unequal error protection with hybrid signal set partition.

PROBLEMS

19.1 Prove that the minimum squared Euclidean distance of the 3-level 8-PSK code given in Example 19.1 is equal to 4.

19.2 Construct a 3-level 8-PSK code with the following three binary component codes: (1) C_1 is the (16, 1, 16) repetition code; (2) C_2 is the (16, 11, 4) second-order RM code; and (3) C_3 is the (16, 15, 2) single parity code.

- **a.** Determine the spectral efficiency of the code.
- **b.** Determine the minimum squared Euclidean, symbol, and product distances of the code.
- **c.** Analyze the trellis complexity of the code.

19.3 Decode the 3-level 8-PSK code constructed in Problem 19.2 with a single-stage Viterbi decoding, and compute its error performance for an AWGN channel.

19.4 Replace the first component code C_1 in Problem 19.2 with the first-order (16, 5, 8) RM code. Construct a new 3-level 8-PSK code. Determine its spectral efficiency, minimum squared Euclidean, symbol, and product distances. Analyze its trellis complexity.

19.5 Decode the code constructed in Problem 19.4 with a three-stage soft-decision decoding. Each component code is decoded with Viterbi decoding based on its trellis. Compute its error performance for an AWGN channel.

19.6 Design a single-level concatenated coded modulation system with the NASA standard (255, 223) RS code over $GF(2^8)$ as the outer code and a 3-level 8-PSK code of length 16 as the inner code. The inner code is constructed using the following binary codes as the component codes: (1) C_1 is the (16, 1, 16) repetition code; (2) C_2 is the (16, 15, 2) single-parity-check code; and (3) C_2 is the (16, 16, 1)

universal code. What is the spectral efficiency of the overall system? Decode the inner code with a single-stage Viterbi decoding and the outer code with an algebraic decoding. Compute the error performance of the system for an AWGN channel.

BIBLIOGRAPHY

1. H. Imai and S. Hirakawa, "A New Multilevel Coding Method Using Error-Correcting Codes," *IEEE Trans. Inform. Theory*, 23 (3): 371–76, May 1977.

2. V. V. Ginzburg, "Multidimensional Signals for a Continuous Channel," *Probl. Peredachi Inform.*, 20 (1): 28–46, 1984.

3. S. I. Sayegh, "A Class of Optimum Block Codes in Signal Spaces," *IEEE Trans. Commun.*, 30 (10): 1043–45, October 1986.

4. R. M. Tanner, "Algebraic Construction of Large Euclidean Distance Combined Coding Modulation Systems," *Abstracts of Papers, IEEE Int. Symp. Inform. Theory*, Ann Arbor, Mich., October 6–9, 1986.

5. G. J. Pottie and D. P. Taylor, "Multilevel Channel Codes Based on Partitioning," *IEEE Trans. Inform. Theory*, 35 (1): 87–98, January 1989

6. A. R. Calderbank, "Multilevel Codes and Multistage Decoding," *IEEE Trans. Commun.*, 37 (3): 222–29, March 1989.

7. T. Kasami, T. Takata, T. Fujiwara, and S. Lin, "On Linear Structure and Phase Rotation Invariant Properties of Block 2^l-PSK Modulation Codes," *IEEE Trans. Inform. Theory*, 37 (1): 164–67, January 1991.

8. T. Kasami, T. Takata, T. Fujiwara, and S. Lin, "On Multilevel Block Modulation Codes," *IEEE Trans. Inform. Theory*, 37 (4): 965–75, July 1991.

9. J. Wu and S. Lin, "Multilevel Trellis MPSK Modulation Codes for the Rayleigh Fading Channels," *IEEE Trans. Commun.*, 41 (9): 1311–18, September 1993.

10. G. D. Forney, Jr., "Coset Codes II: Binary Lattices and Related Codes," *IEEE Trans. Inform. Theory*, 34 (5): 1152–87, September 1988.

11. T. Takata, S. Ujita, T. Kasami, and S. Lin, "Multistage Decoding of Multilevel Block MPSK Modulation Codes and Its Performance Analysis," *IEEE Trans. Inform. Theory*, 39 (4): 1204–18, July 1993.

12. T. Woerz and J. Hagenauer, "Multistage Coding and Decoding for a MPSK System," *Proc. IEEE Global Telecommun. Conf.*, pp. 698–703, San Diego, Calif., December 1990.

13. T. Kasami, T. Takata, T. Fujiwara, and S. Lin, "A Concatenated Coded Modulation Scheme for Error Control," *IEEE Trans. Commun.*, 38 (6): 752–63, June 1990.

14. D. J. Rhee and S. Lin, "Multilevel Concatenated Coded M-DPSK Modulation Schemes for the Shadowed Mobile Satellite Communication Channel," *IEEE Trans. Vehicular Tech.*, 48 (5), 1634–49, September 1999.

15. G. D. Forney, Jr., "Approaching the Capacity of the AWGN Channel with Coset Codes and Multilevel Coset Codes," *Proc. IEEE Int. Symp. Inform. Theory*, p. 164, June 29–July 4, 1997.

16. U. Wachsmann, R. F. H. Fischer, and J. B. Huber, "Multilevel Codes: Theoretical Concepts and Practical Design Rules," *IEEE Trans. Inform. Theory*, 45 (5): 1361–91, July 1999.

17. S. Rajpal, D. J. Rhee, and S. Lin, "Low-Complexity and High-Performance Multilevel Coded Modulation for the AWGN and Rayleigh Fading Channels," *Information Theory*, edited by T. A. Gulliver, Springer-Verlag, New York, 1994.

18. S. Rajpal, D. J. Rhee, and S. Lin, "Coded MPSK Modulations for the AWGN and Rayleigh Fading Channels," *Communications, Coding, and Cryptography*, edited by R. Blahut, D. J. Costello, and S. Mauer, Kluwer Academic, Bosten, Mass., 1994.

19. D. J. Rhee, S. Rajpal, and S. Lin, "Some Block- and Trellis-Coded Modulations for the Rayleigh Fading Channel," *IEEE Trans. Commun.* 44 (1): 34–42, January 1996.

20. S. Rajpal, D. J. Rhee, and S. Lin, "Multidimensional Trellis Coded Phase Modulation Using a Multilevel Concatenation Approach, Part I: Code Design," *IEEE Trans. Commun.*, 45 (1): 64–72, January 1997.

21. S. Rajpal, D. J. Rhee, and S. Lin, "Multidimensional Trellis Coded Phase Modulation Using a Multilevel Concatenation Approach, Part II: Codes for the AWGN and Fading Channels," *IEEE Trans. Commun.*, 45 (2): 177–86, March 1997.

22. S. Rajpal and S. Lin, "Product Coded Modulation," *IEEE Trans. Commun.*, 45 (4): 389–92, April 1997.

23. S. Wainberg, "Error-Erasure Decoding of Product Codes," *IEEE Trans. Inform. Theory*, 8: 821–23, November 1972.

24. B. Masnick and J. K. Wolf, "On Linear Unequal Error Protection Codes," *IEEE Trans. Inform. Theory*, 13 (4): 600–607, October 1967.

25. A. R. Calderbank and N. Seshadri, "Multilevel Codes for Unequal Error Protection," *IEEE Trans. Inform. Theory*, 39 (4): 1234–48, July 1993.

26. L. F. Wei, "Coded Modulation with Unequal Error Protection," *IEEE Trans. Commun.*, 41 (10): 1939–49, October 1993.

27. R. H. Morelos-Zaragoza, M. P. C. Fossorier, S. Lin, and H. Imai, "Multilevel Coded Modulation for Unequal Error Protection and Multistage Decoding—Part I: Symmetric Constellations," *IEEE Trans. Commun.*, 48 (2): 204–13, February 2000.

28. M. Isaka, M. P. C. Fossorier, R. H. Morelos-Zaragoza, S. Lin, and H. Imai, "Multilevel Coded Modulation for Unequal Error Protection and Multistage Decoding—Part II: Asymmetric Constellations," *IEEE Trans. Commun.*, 48 (5): 2774–86, May 2000.

29. E. Biglieri, D. Divsalar, P. J. McLane, and M. K. Simon, *Introduction to Trellis-Coded Modulation with Applications*, Macmillan, New York, 1991.

30. G. Ungerboeck, "Channel Coding with Multilevel/Phase Signals," *IEEE Trans. Inform. Theory*, 28 (1): 55–67, January 1982.

31. C. Schlegel and D. J. Costello, Jr., "Bandwidth Efficient Coding for Fading Channel: Code Construction and Performance Analysis," *IEEE J. Select. Area Commun.*, 7 (9): 1356–68, December 1989.